APPLICATIONS OF POLY (3-HEXYLTHIOPHENE) THIN FILM AS A

HYDRAZINE-SENSITIVE CHEMIRESISTOR

Except where reference is made to the work of others, the work described in this thesis is my own or was done in collaboration with my advisory committee. This thesis does not include proprietary or classified information.

_____
Huihua Shu

Certificate of Approval:

_____   _____
Zhongyang Cheng   Bryan A. Chin, Chair
Assistant Professor   Professor and Chair
Materials Engineering   Materials Engineering

_____   _____
Dong-Joo Kim   Stephen L. McFarland
Assistant Professor   Acting Dean
Materials Engineering   Graduate School

APPLICATIONS OF POLY (3-HEXYLTHIOPHENE) THIN FILM AS A

HYDRAZINE-SENSITIVE CHEMIRESISTOR

Huihua Shu

A Thesis

Submitted to

the Graduate Faculty of

Auburn University

in Partial Fulfillment of the

Requirement for the

Degree of

Master of Science

Auburn, Alabama
Dec 15, 2006

APPLICATIONS OF POLY (3-HEXYLTHIOPHENE) THIN FILM AS A

HYDRAZINE-SENSITIVE CHEMIRESISTOR

Huihua Shu

_____

Signature of Author

_____

Date of Graduation

VITA

Huihua Shu, daughter of Jingguo Shu and Linzhu Li, was born on March 12, 1981, in Shanghai, China. She received her Bachelor of Science degree in Materials Science and Engineering from Shanghai Donghua University, China, in June 2003. She then entered the Auburn University in August 2003 for the degree of Master of Science in Materials Engineering.

THESIS ABSTRACT

APPLICATIONS OF POLY (3-HEXYLTHIOPHENE) THIN FILM AS A

HYDRAZINE-SENSITIVE CHEMIRESISTOR

Huihua Shu

Master of Science, Dec 15, 2006
(B.S. Donghua University, China, June 2003)

112 Typed Pages

Directed by Bryan A Chin

Hydrazine is a hypergolic compound that when combined with mixed oxides of nitrogen self ignites. This compound is used for the steering (guidance and course correction) of satellites and spacecraft. Hydrazine is a highly toxic and carcinogenic species exhibiting toxic effects in humans at very low levels of exposure. Both the American Conference of Government Industrial Hygienists (ACGIH) and the Air Force Office of Safety and Health (AFOSH) have set the hydrazine exposure threshold limit value (TLV) to 10 ppb in air for an 8-hour period. Hence a sensor capable of hydrazine detection at the ppb level is required to protect individuals working around device containing hydrazine. In this thesis, a type of passive, low cost, Poly (3-Hexylthiophene) (P3HT) thin-film chemiresistor micro-sensor was fabricated and investigated for the detection of hydrazine and associated compounds. The sensor works on the principle that interaction with hydrazine reduces the number of charged couple pairs in the P-type

doped P3HT thin film. This causes the thin film to undergo a permanent and large increase in resistance.

Standard microelectronic manufacturing techniques were used to form a micro-sensor composed of silicon substrate, interdigitated gold electrodes, and P3HT sensing film. Responses of the micro-sensor to hydrazine at different temperatures and concentration levels are reported. The effect of different doping levels of P3HT thin film was investigated to improve the sensor stability. Thermally-induced effects on performance and thermal stability of the P3HT thin film micro-sensor are also explored. The experiments show that the micro-sensor resistance increases from 1 to 2 ohms to over 10^6 ohms upon exposure to 25 ppm concentration of hydrazine at a flow rate of 4 liters/min. Experiments also showed that the sensor's sensitivity to hydrazine vapor at low concentration levels can be enhanced by thermal treatment. In addition, thermally annealed and heavily doped P3HT micro-sensors had better thermal stability at high temperature. The sensors exhibited good specificity to hydrazine with no response to NO2 and N_2O.

ACKNOWLEDGEMENTS

The author would like to extend her deepest thanks to Dr. Bryan A. Chin, professor and chairman of Materials Engineering, for his supervising this thesis and being a great academic advisor during the author's graduate study at Auburn University.

The author would like to express her appreciation to committee members, Dr. Zhongyang Cheng and Dr. Dong-Joo Kim in Materials Engineering for their great help and discussion.

The author is also grateful to staff members and colleagues in Materials Engineering, and Mr. Charles Ellis in Electrical and Computer Engineering, for their kind help.

Finally the author would like to thank her parents, for their love, support and encouragement.

Style manual or journal used: <u>Bibliography conforms to those of the transactions of the</u>

<u>Institute of Electrical and Electronics Engineers</u>

Computer software used: <u>Microsoft Office 2003</u>

TABLE OF CONTENTS

LIST OF FIGURES

xiii

xiv

LIST OF TABLES

CHAPTER 1

INTRODUCTION AND THEORY

1.1   Background

The detection and monitoring of various chemical gases are very important for many applications. One major application area is industrial monitoring, especially in industries dealing with beverages, food processing and other chemical products [1, 2]. Another vital area is environmental monitoring, where it is crucial to be able to detect both the presence and the concentration of dangerous or toxic gases generated by leaks and spills [3].

Chemical sensors are therefore important to all aspects of modern life, since these devices monitor chemical manufacturing, industrial materials processing, protect the natural environment, and improve the safety of human beings in the workplace [4].

A chemical sensor is a measurement system designed to generate an experimental response that is proportional to the quantity of a specific sensed chemical species. It can be designed to respond to a sample of the species contained within a known small volume, or to measure the species directly in bulk liquid, solid or gaseous samples [5]. Chemical sensors are classified into various types according to the sensing principle by which they detect the chemical measurand. The general types of sensors, along with the operating principle and a typical example of a chemical sensor of each type, are listed in Table1-1.

Table1-1   Principle, measurands and examples of chemical sensors

Principle	Measurand	Example
Conductometric	Conductance/Resistance	Oxide gas sensor
Capacitive	Capacitance/Charge	Polymer humidity sensor
Resonant	Frequency	Surface Plasmon
Gravimetric	Mass	Piezoelectric /Saw sensor
Amperometric	Current	Electrochemical cell

The selectivity of the chemical sensor is mainly dependent on its reaction mechanism. A sensor should preferably only be responsive to a single chemical, even in the presence of others. This selectivity (response to only one chemical species) can be obtained through the choice of a suitable sensing material [6].

Recent improvements in chemical sensors result from advances in the availability of new materials and advanced microfabrication techniques, which have made possible a greater degree of miniaturization and energy efficiency. High performance sensors fabricated by integrating sensing devices with different sensing characteristics have been investigated and developed for critical applications, where a double or even triply redundant (self-checking) system is often used in situations where the failure of an alarm or gas detector may lead to permanent injury or death of personnel [7].

1.2   Overview of Conducting Polymer-based Chemiresistors

1.2.1   Chemiresistors

Although many chemical sensors are widely used commercially for field measurements of chemical species, few have been successfully applied to geologic environments for long term monitoring [8]. The chemiresistor sensor, which is a type of chemical sensor representing a conceptually very simple electronic approach to detecting chemical species in the gas phase, is potentially very useful for environmental monitoring. A chemiresistor sensor is usually composed of the insulating substrate, patterned electrodes and a gas sensitive layer. Figure 1-1 shows the schematic arrangement of a typical chemiresistor [6]. Changes in the resistance of an organic or inorganic material in

V

I

Gas

Sensing material

Electrodes

SiO$_2$

Si
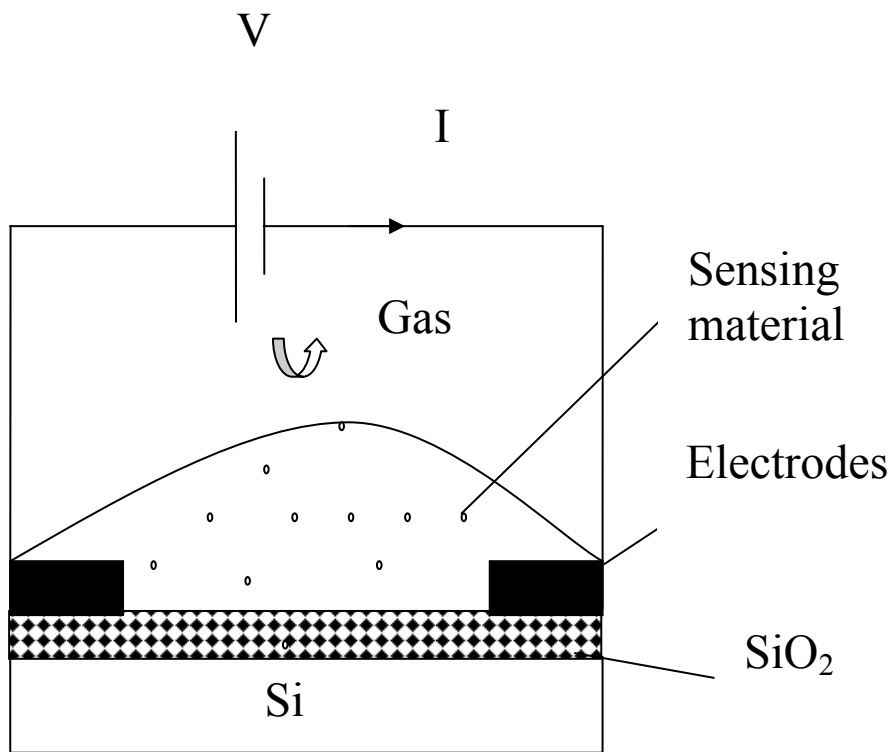
Figure1-1   General structure of a chemiresistor gas sensor

response to an analyte gas provide the primary mechanism for gas detection. Therefore, the material for the gas sensitive layer, which determines the specificity and sensitivity for the gas of interest, becomes the critical component in the sensor. This sensing material must be electrically conducting and is usually applied as a continuous film. Three kinds of materials, namely organic crystals, metal oxides and conducting polymers, have been investigated for possible use in this sensing film. Amongst these, conducting polymers have attracted the most interest since their first discovery in the 1980s [6].

1.2.2 Conducting Polymers

Many applications of conducting polymers, which combine the electrical properties of metals with those of processible plastics, have been successfully used for more than ten years in electronic, mechanical and chemical microsystems such as sensors, electrolytic capacitors, battery electrodes, electrostatic loudspeakers and magnetic storage media [9, 10]. Today, the application of conducting polymers in microsystems is attracting particular interest due to the special features inherent in the chemical structure of their monomers and their advantageous chemical, and physical properties [11].

Conducting polymers are a new class of organic polymers that can be electrically synthesized from aromatic heterocyclic monomers. Conducting polymers have an extended p-orbital system through which electrons are able to move from one end of the polymer to the other [6]. Many studies have already investigated the basic structures and principles of conducting polymers [12]. Most are conjugated polymers, which allow the existence of highly delocalized states. The basic structural characteristic of all these conjugated polymers is their quasi-infinite π system that extends over a large number of

continuous monomer units. This structure gives these materials a directional conductivity along the axis of the chain [13].

Conducting polymers are extensively conjugated molecules that have a spatially delocalized, band-like electronic structure [14]. Based on band theory, in order to be electrically conducting the polymer must have a continuous system of strongly interacting atomic orbitals that lead to a closely spaced electronic state. However, the conduction in electrically conducting polymers is not related to their intrinsic semiconductor properties and they still act as insulators until they react with reducing or oxidizing agents. Oxidation or reduction of the polymer creates a charged unit called a bipolaron on the chain (see Figure 1-2). From an electrochemical perspective, the most important aspect of conducting polymers is their ability to act as electronic conductors.

Conducting polymers act as electron donors when exposed to reducing agents and electron acceptors when exposed to oxidizing agents. These two processes are called n-type doping and p-type doping, respectively (see Figure 1-3). N-doping introduces freely moving electrons into the conduction band, while p-doping removes electrons from the valance band and creates holes to allow other electrons to move into. The conductivity of a conducting polymer increases quickly and then becomes stable at a maximum value when it is exposed to either p-type or n-type doping agents [9]. Once the polymer has been doped by oxidizing or reducing agents, they can be transformed from an insulating material to a conducting material or vice versa [15].
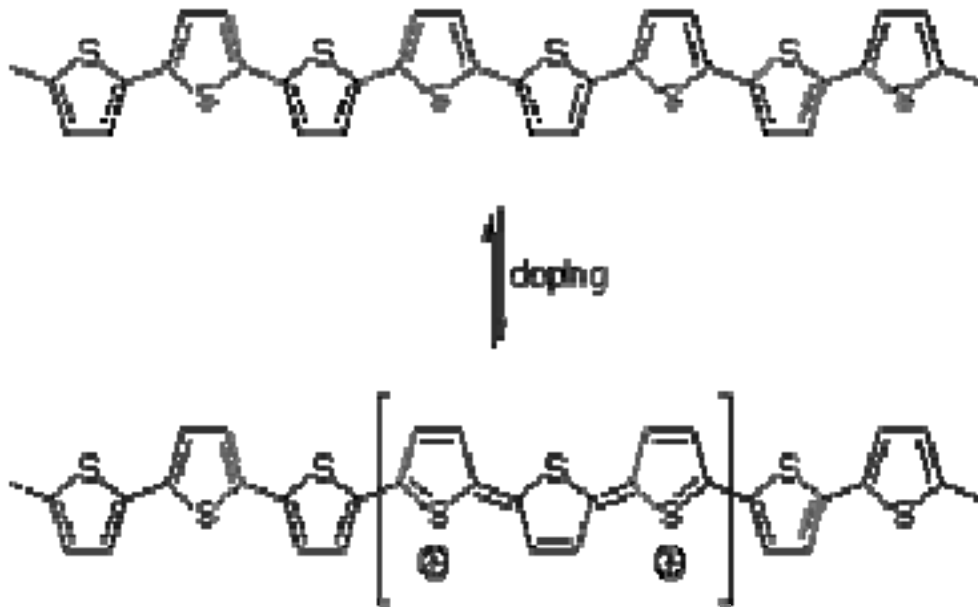
Figure 1-2   Removal of two electrons (p-doping) from a Polythiophene chain produces a bipolaron [15]

P-Type Doping
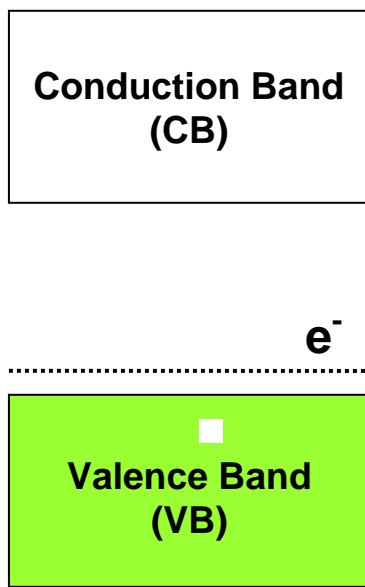
N-Type Doping
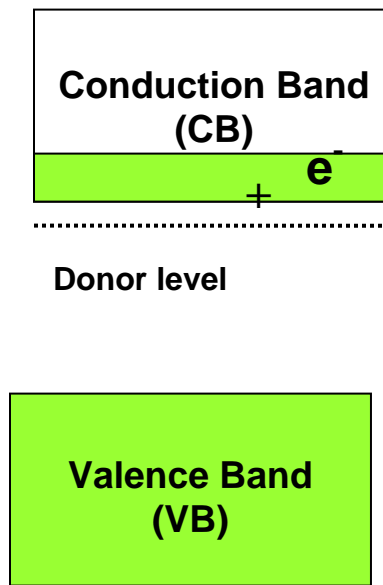
Figure1-3   P-type and N-type doping of inorganic semiconductor

1.2.3 Application of Conducting Polymers in Chemiresistor Sensors

In recent years, more attention has been focused on the application of conducting polymers as the sensitive layer in chemiresistor sensors for the detection of organic vapors. When a conducting polymer interacts with different species, its electronic conductivity, which is related to its redox state, will change accordingly. These changes in the conducting polymer's properties, for example, its current and resistance, provide a straightforward and easily read sensor response [16].

Conducting polymers offer many advantages over other gas-sensing materials such as organic crystals and metal oxides. Not only do conducting polymers respond to a wide range of organic vapors, but they respond at room temperature, unlike metal oxides, which require very high temperatures of around 300~400°C to act as suitable sensors. Conducting polymers are also highly sensitivity to different organic compounds at the ppb to ppm levels [17, 18]. The responses of many conducting polymers to a broad range of organic vapors or odors have been investigated. A common feature of the most promising of these polymers is the presence of a conjugated π-electron system extending over the whole polymer backbone. The most commonly used polymers in gas sensors are those based on n-methylpyrrole, pyrrole, and thiophene monomers (see Figure 1-4). These heteroaromatic monomers undergo electrochemical oxidation to form conducting polymer films that can be deposited over interdigitated electrodes to make gas-sensitive chemiresistors [6, 18, 19].

When a conductive polymer interacts with a specific gas, it can act either as an electron acceptor or a donor. The hole conductivity of a p-type conducting polymer
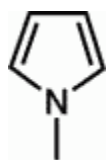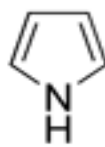
n-methylpyrrole   **pyrrole**   **thiophene**

Figure 1-4   Chemical structures of some common monomers

increases if it donates electrons when reacting with the gas, while the conductivity decreases if it acts as electron acceptor. In addition to this change in the number of charged carriers, there is also a change in the bulk mobility of the conducting polymer due to changes in the conformation of the polymer backbone. However, the inherently long time constant, which is usually accompanied by some degree of hysteresis, is a major disadvantage of responses originating in the bulk of the conducting polymer. These effects are caused by the slow penetration of gases into conducting polymers, and the secondary doping induces a modulation of carrier number, mobility and their contribution to the whole change of conductivity varies [19]. Since conducting polymers are sensitive to a wide range of polar molecules at room temperature and many reports have already indicated that a sensitivity down to 0.1 ppm is possible, these conducting polymers are potentially a very important material for new applications in low-concentration gas sensing [6].

1.3   Hypergolic Vapor Detection

Large quantities of hypergolic compounds, including hydrazine (HZ), monomethylhydrazine (MMH), and unsymmetrical dimethylhydrazine have been widely used in the steering (guidance and course correction) of satellites and spacecraft. When these hypergolic compounds come into contact with oxidizing compounds, they ignite spontaneously, without an external ignition source. This easy ignition and reignition property of hypergolic compounds makes them ideal for spacecraft maneuvering systems [20]. Additionally, hydrazine compounds are generally powerful reducing agents due to their high hydrogen content, and the combustion by-products are nitrogen. Hydrazine

compounds are used to remove corrosive products and contaminants in the heat transfer systems of nuclear and coal fired power generation plants and also to recover elements such as silver and nickel from metal salts left over from mining and manufacturing processes [21].

However, hydrazine compounds are both highly toxic and carcinogenic species, exhibiting toxic effects in humans at very low levels of exposure. The American Conference of Government Industrial Hygienists (ACGIH) has set the hydrazine exposure threshold limit value (TLV) to 0.01 parts-per million (ppm) TWA (time-weighted average) [21]. These very low levels of required detection pose a special challenge for the sensors that are used to monitor the possible leakage of hydrazine in stored missiles. Missiles may be stored underground for up to 10 years, with no access to a power source that can be utilized to actively monitor and record hydrazine levels. In these cases a passive (no-power) sensor is required that would indicate that a hydrazine leak had occurred. Hydrazine leaks are not only dangerous to personnel, but may seriously damage missile components. Personnel moving the missile must be able to assess the safety of both the missile and the environment in which they are working. For these applications, a passive sensor that undergoes a permanent change when exposed to hydrazine is desirable.

Several methods have been developed for the detection of low levels of hydrazine compounds, including colorimetric methods, coulometric techniques, mass spectrometric methods, electrochemical detectors and chemiluminescence detectors. However, each of these methods has one or more disadvantages that limit their applications. For example, some methods involve a wet chemical step are discontinuous, or do not analyze the

vapours in the gaseous state but require collection of the vapours in the liquid state. Many detectors lack selectivity, and often respond to other common airborne compounds such as oxygen, carbon dioxide, and organic compounds. Other drawbacks are expense, operator expertise, and detector life-time limitations [21, 22, and 23]. Therefore, there is an urgent need for an improved method for hydrazine compound vapour detection that is accurate, simple, specific, cost-effective, and sensitive.

1.4 Poly(3-Hexylthiophene) Thin Film Hydrazine Sensor

Two types of hydrazine sensors are currently used. The first, the electrochemical hydrazine sensor, has a short life time (approximately 1 year) but requires a continuous current of only 100 mA to operate. The other type of commercially available hydrazine sensor is the solid state hydrazine sensor, which has a longer life time (3 years) but requires a higher continuous current of 250~350 mA. The detection limit of these sensors is around one to five ppm of hydrazine in air, which is three orders of magnitude above the desired threshold. Therefore, the investigation of a new type of hydrazine micro-sensor with very high sensitivity is required.

1.4.1 Poly (3-hexylthiophene) Conducting Polymer

Regioregular poly (3-hexylthiophene) (RR-P3HT) was used as the sensitive thin film layer in this research. This polymer is of fundamental and industrial interest for use as the active material applied in organic semiconductor devices [24-26]. It is one of the most promising conducting polymers and belongs to the class of hole-conducting, conjugated polymers. It is easily processed and has a high charge carrier mobility, easy

synthesis, environmental stability, and self-assembling properties [27]. Due to its high degree of internal ordering, RR-P3HT also exhibits excellent electrical properties, good environmental stability, and better electroconductivity than other conducting polymers. Figure 1-5 schematically shows the chemical structure of regioregular head to tail (HT) Poly (3-hexylthiophene). The head-to tail regiospecific conformation of RR-P3HT makes up over 98.5% of the bulk material. Details about the synthesis procedures and characteristics of RR-P3HT can be found in Ref. [28].

1.4.2 Oxidation of poly (3-hexylthiophene) Thin Film

In this study, P3HT thin film was doped using nitrosonium hexafluorophosphate (NOPF6)/acetonitrile solution, which acts as an oxidizing agent. NOPF6 was chosen as the dopant because the doped P3HT thin films produced are highly stable and respond reproducibly to hydrazine gas [9]. Upon initial doping, polarons are created. Further doping of the polymer creates a bipolaron. At even higher levels of doping, the biopolaron energies will overlap to create narrow bipolaron bands within the band gap. In the oxidation process of Poly (3-hexylthiophene), shown in Figure 1-6, an electron is removed from the π-system of the neutral polymer chain to an acceptor, creating a free unpaired electron and a fixed positive charge. In order to compensate for these two defects on the polymer backbone, several denzoid-like rings are locally changed to quinoid-like rings. A polaron can be described as a group of a positive charge site tied to a free unpaired electron through a local lattice distortion, which creates new localized electronic states that reside in the energy gap symmetrically. The lower energy states are occupied by unpaired electrons. When continuing the doping process, the free unpaired

14
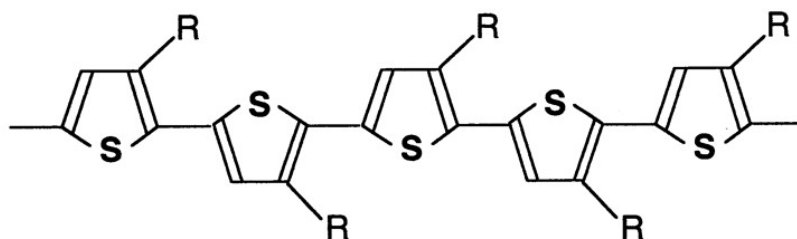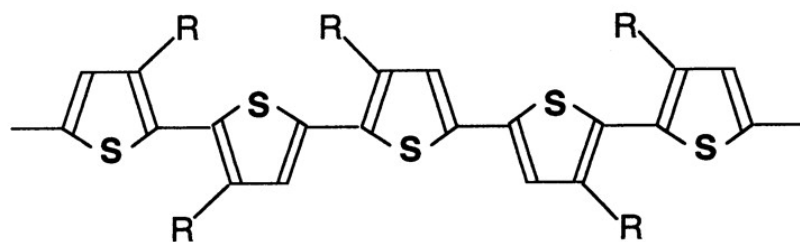
(a) Regioregular(RR)

(b) Regiorandom (RRa)

Figure 1-5   (a)   Regioregular and (b) Regiorandom stereo orders of P3AT polymer chains. R, alkyl group; S, sulfur [29].
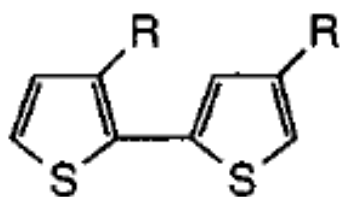
Head to tail (HH)   Head to Head (HH)

$R = C_6H_{13}$
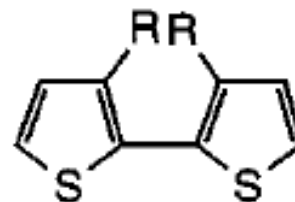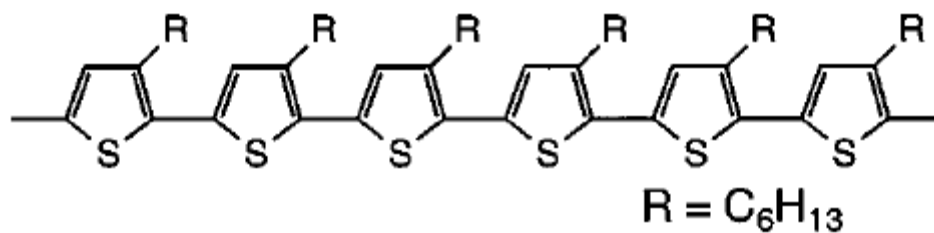
Figure 1-5 (c) Chemical Structure of head-to-tail regioregular Poly (3-hexylthiophene) [24]
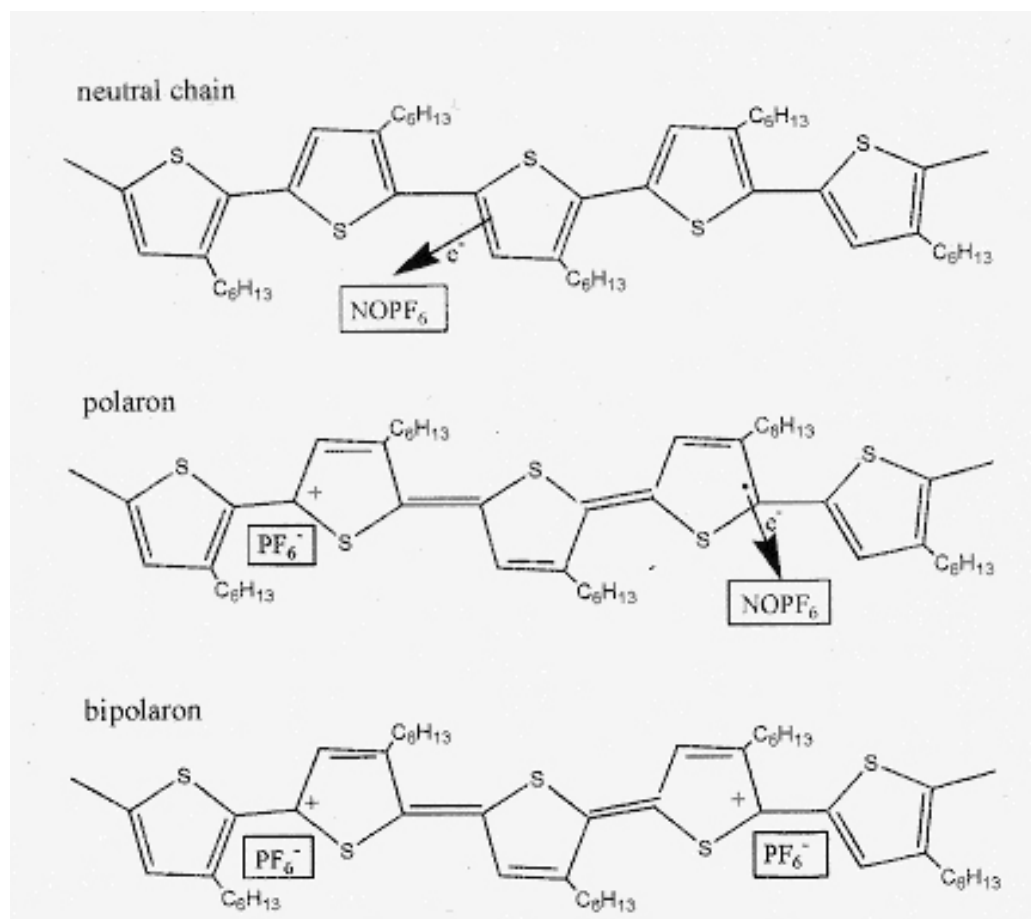
Figure 1-6   Poly (3-hexylthiophene) oxidation process [30]

electron in the polaron are removed to an acceptor, creating the biopolaron, which is defined as the combination of two positive charge sites and a local lattice distortion. Further doping will cause the localized bipolaron states to merge to form bipolaron bands. Figure 1-7 presents the energy levels that are associated with polarons and bipolarons [9,12, 30].

1.4.3 The Stability of poly (3-hexylthiophene) Conducting Polymer

The stability of conducting polymers is a critical factor from the point of view of industrial applications. The stability of conducting polymers has been actively investigated by many researchers over several years. Regioregular poly (3-hexylthiophene) is one of the p-type semiconducting materials with low ionization potential, and it is known to form a reversible charge-transfer complex with oxygen [31]. These p-type semiconducting materials are able to exhibit large positive threshold voltage shifts (V_T) upon exposure to air, presumably due to the polymer doping [32]. However, poly (3-hexylthiophene) has poor photostability when it is exposed to intense light in the presence of oxygen, which decreases the field effect mobility and corresponds to a reduction of the conjugation within the poly (3-hexylthiophene) [33]. According to previous studies, the oxidation stability of poly (3-hexylthiophene) can be improved by increasing the ionization potential of the polythiophene backbone [34]. However, more detailed studies are needed to systematically understand the effects on the stability of poly (3-hexylthiophene) and determine the best way to improve the stability. In this research, stability tests of NOPF6 doped poly (3-hexylthiophene) thin film micro-sensor were conducted as a function of time under controlled environments.

Energy

Neutral Chain	Polaron	Bipolaron	Bipolaron Bands

Conducting band   Valence band
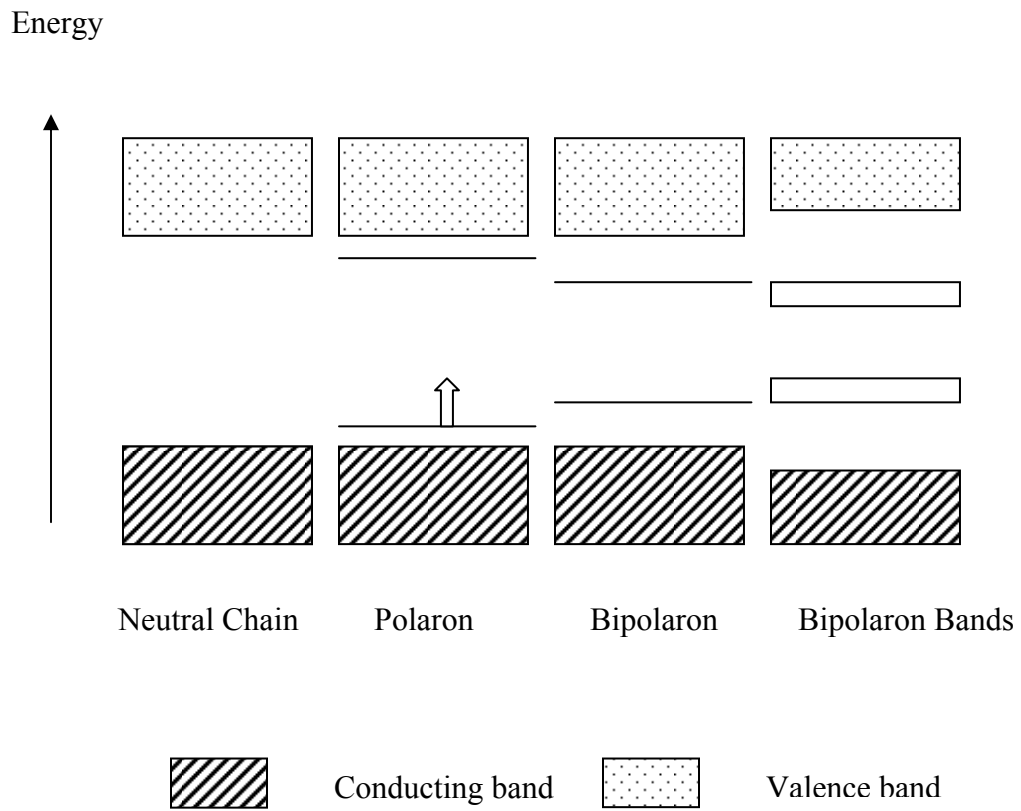
Figure 1-7   Polaron and bipolaron states in the energy gap [9,12]

1.5   Objective

The goal of this thesis is to develop and investigate a new poly (3-Hexylthiophene) thin film-based chemiresistor micro-sensor to detect hydrazine at parts-per-billion (ppb) to parts-per-million (ppm) concentration levels at ambient pressure. The main focus of this research is the improvement of the sensitivity at ppb hydrazine exposure levels and the improvement of the thermal stability over the temperature range -50˚C to 70˚C. Thermal treatment and different doping methods (to increase the initial number of mobile charge carriers) of the P3HT thin film are also investigated in order to alter the polymer structure and improve the sensitivity, stability and efficiency of the micro-sensor.

CHAPTER 2

SENSOR FABRICATION AND EXPERIMENTAL PROCEDURE

A miniature Poly (3-Hexylthiophene) (P3HT), thin-film-based, chemiresistor sensor fabricated on silicon using micromachining technology is developed in this research for hydrazine gas sensing applications. The micro-sensor is composed of P3HT sensing film, gold interdigitated electrodes and oxidized silicon substrate. Figure 2-1 shows the schematic structure of the P3HT-based chemiresistor micro-sensor.   The experimental procedures of interdigitated electrode fabrication, polymer deposition, hydrazine exposure tests, stability tests, and characterization of the sensing film will be discussed in this chapter.

2.1   Preparation of P3HT-based Micro-sensor

2.1.1   Materials

The sensor is based on a single-side, polished, p-type, boron doped silicon (100) wafer.   The diameter, thickness and resistivity of this wafer is separately 100mm, 500~550um, and 0.01-0.02 ohm-cm. All the silicon wafer fabrication processes were completed at the Alabama Microelectronics Science and Technology Center (AMSTC).

P3HT thin film

SiO₂ substrate

Gold Pads

Gold interdigitated electrode pairs
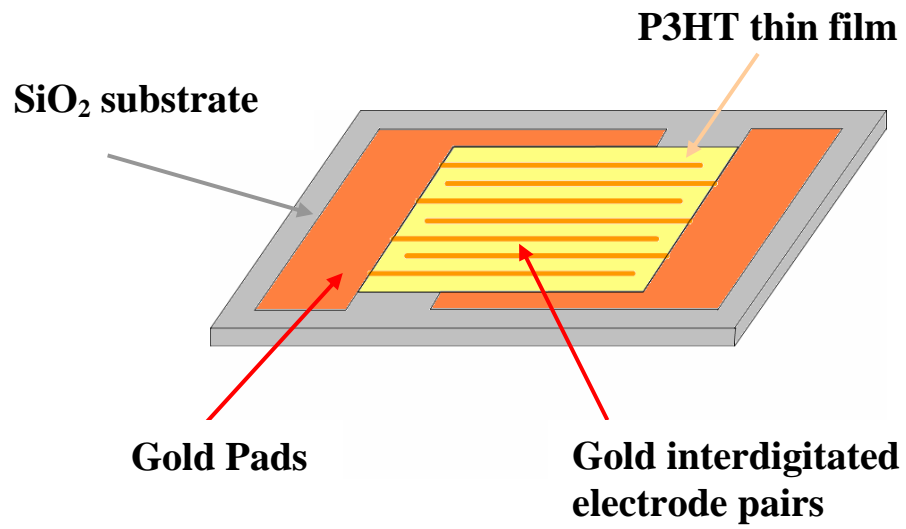
Figure 2-1   (a) Schematic of a P3HT-based chemiresistor micro-sensor

Interdigitated electrodes

P3HT thin film

Silicon dioxide
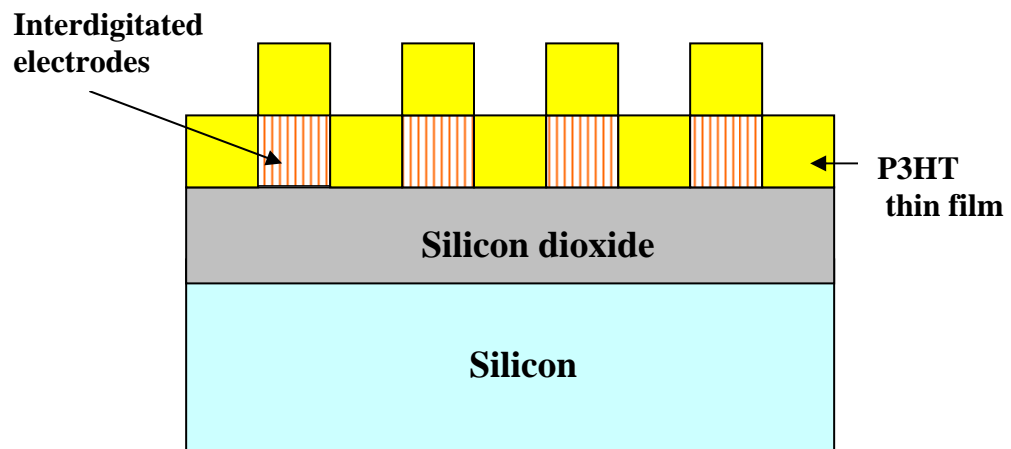
Silicon

Figure 2-1   (b) Side view of a P3HT-based chemiresistor micro-sensor

2.1.2 Sensor geometry

The chemiresistor sensor designed in this research was mainly composed of a set of gold interdigitated electrodes on a silicon substrate (Figure 2-2). Table 2-1 specifies the parameters used in this sensor design. The geometry of the sensor pattern (see Figure 2-3) was designed using the "LASI 7" software and a final positive photomask was produced on a glass plate.
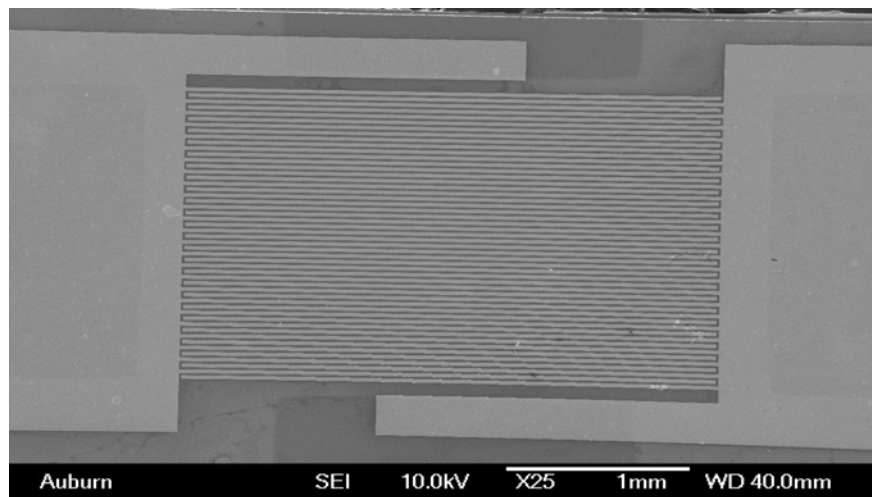
Fig 2-2   Gold interdigitated electrode pairs

24

Table 2-1   Parameters of the sensor geometry

Number of electrode pairs	25
Width of electrode finger	22 um
Length of electrode finger	2985 um
Space between fingers	15 um
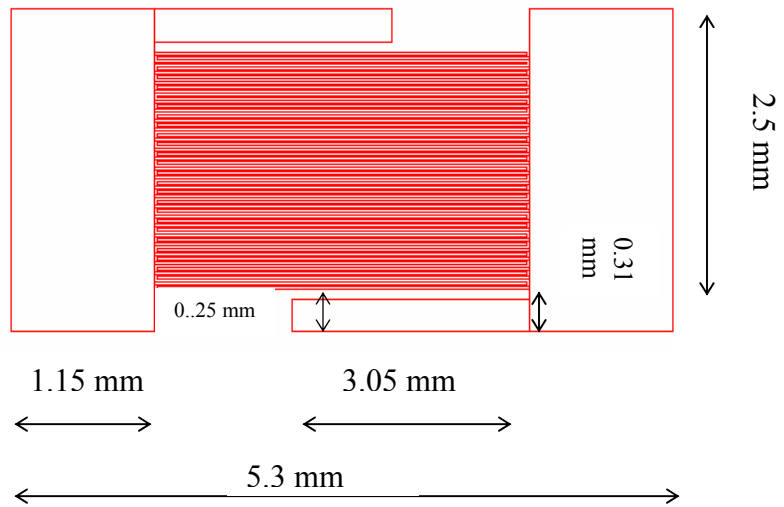
Figure 2-3   Geometry of the sensor pattern

2.1.3 Fabrication procedures of micro-sensor

The fabrication process of the micro-sensor is composed of the steps listed below and the process sequences are shown in the Figure 2-4.

1) Wafer cleaning: Prior to use, the 4 inch wafer was first chemically cleaned to remove ionic, organic, or metallic impurities from the silicon surface. Table 2-2 details a typical cleaning process applied in this research. Throughout the wafer cleaning and the microelectronic fabrication process, deionized (DI) water was used to remove all traces of contamination [35].

2) Barrier formation: After wafer cleaning, a layer of Silicon dioxide (SiO_2) was formed on the silicon wafer surface acting as a barrier layer. This SiO_2 barrier layer was produced using thermal oxidation. The wafers were thermally oxidized in a furnace at 1000^oC under one atmosphere of pure oxygen for 2 hours. The thickness of the oxidation layer was measured to be 7201 Å and the colour of wafer surface was blue green.

3) Photoresist Application and soft baking: A layer of light sensitive photoresist was coated onto the oxidized surface of the wafer using the spin coating method. The wafer was first held on a vacuum chunk and then spun at 3000 rpm for 30 seconds to obtain a 1 um thick uniform layer. In order to ensure good photoresist adhesion, the wafer surface was exposed to hexamethyldisilazane (HMDS) for 20 minutes prior to the spin coating. After the photoresist application, the wafer was soft baked at 105^oC for 1 minute to remove all the solvents from the photoresist coating.

27

4) Mask Alignment and Exposure: The mask was aligned with the wafer to transfer the designed pattern onto the wafer surface. Once the layout was accurately aligned, the photoresist was exposed through the pattern on the mask with a high intensity ultraviolet light.

5) Development: This is one of the last steps in the photolithographic process. The resist in the patterned area that had been exposed to the ultraviolet light was washed away using a 1:2 developer to water solution for 18 seconds leaving other areas still covered with photoresist. The exposed part without the resist was the exact pattern layout on the wafer surface.

6) Metal film deposition and removal of photoresist: After the photolithography process, the wafer was deposited with the metals, titanium and then gold, using a CHA Industries Mark-50 Electron Beam. The deposition specification is shown in Table 2-3. The metal coated wafer was then cleaned using acetone in an ultrasonic bath, leaving the patterned metal film.

7) Polymer coating and annealing: The wafer was first cleaned by acetone, then ethanol, and DI water. Then, it was coated with a uniform layer of Poly (3-Hexylthiophene) thin film by the spin coating method. After that, the wafer was either annealed at different temperatures in an oven for 1 hour or taken directly to etching.

8) Polymer etching: In order to remove the polymer that coated the gold contacts where wire bonding to the interdigitated electrodes occurs, a wafer with etched holes having the same size and placement of holes as the deposited contact pads was fabricated using the photolithography process and

etched through by ASE (advanced silicon etcher) from Surface Technology Systems (STS) company. This etched wafer was then aligned with the polymer coated wafer using optical microscopy and the polymer on the contact pads was removed using AOE (advanced oxide etcher) from Surface Technology Systems (STS) company. Figure 2-5 shows the actual as-fabricated wafers.

9) Wafer dicing: Finally, the whole wafer was diced into test sensors using a diamond saw having the dimensions of 2.5 mm x 5.3 mm (W x L). The sensors were carefully dried and stored before testing and experiment.

Silicon Wafer

Oxidation

Photoresist

Lithography

Au & Ti deposition

Etch Photoresist

Polymer coating

No-treatment   Annealing

Polymer Etching

Wafer dicing
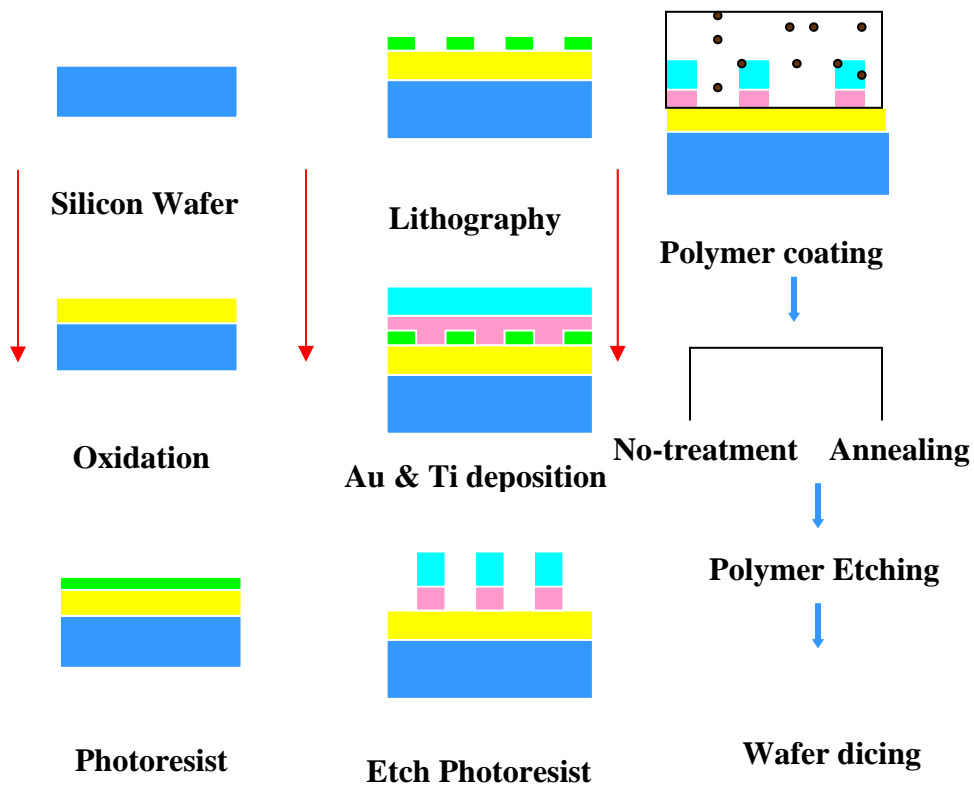
Fig 2-4   Fabrication sequence of P3HT chemi-resistor micro-sensor
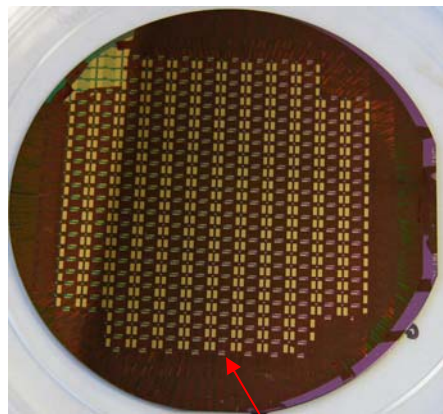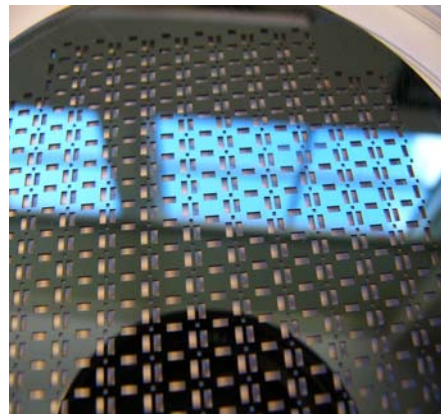
<center>(a)</center> <center>(b)</center>
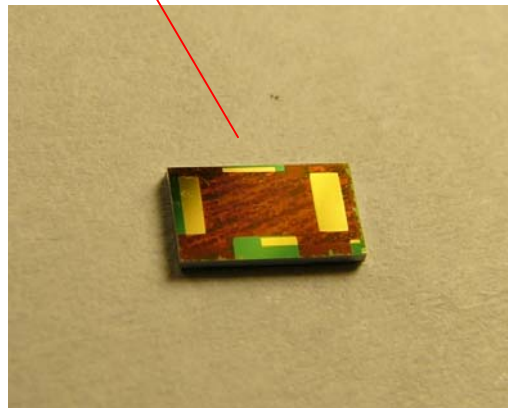
<center>(c)</center>

Fig 2-5   Actual fabricated sensors on the silicon wafer (a) P3HT thin film micro-sensors based on the silicon substrate, (b) Partially etched wafer used to remove polymer adhering to contact bonding pads, and (c) Single P3HT thin film micro-sensor after dicing

Table 2-2   Silicon Wafer Cleaning Procedure [35-37]

A. Solvent Removal
    1. Immerse in boiling trichloroethylene(TCE) for 3 min
    2. Immerse in boiling acetone for 3 min
    3. Immerse in boiling methyl alcohol for 3 min
    4. Wash in DI water for 3 min

B. Removal of Residual Organic/Ionic Contamination
    1. Immerse in a (5:1:1) solution of H_2O-NH_4OH-H_2O_2; heat solution to 75-80°C and hold for 10min
    2. Quench the solution under running DI wafer for 1 min
    3. Wash in DI water for 5 min

C. Hydrous Oxide Removal
    1. Immerse in a (1:50) solution of HF-H2O for 15 sec
    2. Wash in running DI water with agitation for 30sec

D. Heavy Metal Clean
    1. Immerse in a (6:1:1) solution of H_2O-NH_4OH-H_2O_2 for 10min at a temperature of 75-80°C
    2. Quench the solution under running DI water for 1 min
    3. Wash in running DI water for 20 min

Table 2-3   Specification of Metal film deposition

Metal	Crucible#	Emm Current	Voltage	Dep.Rate	Power	Thickness
Ti	1	0.17	8.78	4.0	64%	50nm
Au	2	0.32	9.76	4.0	95%	200nm

2.2 Preparation of Poly (3-hexylthiophene) Thin Film

2.2.1 Poly (3-hexylthiophene) thin film deposition

Poly (3-hexylthiophene) with more than 98.5 regioregularity and an average molecular weight (M_w) of around 87,000 g /mol was purchased from Aldrich. It was mixed at a weight of 20mg/ml in chloroform. The solution was spin-coated in air at 3000 rpm onto the sensor platform using a WS-400B-6NPP/LITE spin coater produced by Laurell Technologies Corporation. The Poly (3-hexylthiophene) thin films used in all of the studies were about 200 nm thick as determined using Alpha-step 200 profilometer from Tencor Instruments.

Various approaches have been developed so far to grow organic or polymer thin films on wafer surfaces with accurate thickness control such as solution casting, aerosol, dip, electrochemical deposition, and spin coating. Of these techniques, the spin coated film is more consistent and has a more planar-like structure when compared with other methods. The polymer solution is deposited onto a spinning surface hence causing the polymer to spread out uniformly from the center.

2.2.2 Poly (3-hexylthiophene) thin film annealing

In order to study the electrical and physical modifications of Poly (3-hexylthiophene) thin film caused by thermal annealing, six inert atmosphere annealing temperatures were explored over the temperature range from 80°C to 220°C. After polymer deposition by the spin coating method, the whole fabricated wafer was directly placed into a Type 47900 furnace manufactured by Barnstead International Corporation for 1 hour annealing at different temperatures prior to dicing.

2.3 Sensor Packaging

In order to make this micro-sensor easier to be handled and more commercially ready for future marketing, we packaged the micro-sensor by wire bonding the sensor chip to the TO-39 header.

Each micro-sensor was first mounted onto the center of the TO-39 header (provided by Sinclair Manufacturing Company) using EP21TCHT-1 epoxy from Master Bond Corporation. This glue is a thermally conductive, heat resistant, epoxy compound that has passed strict outgassing specifications as developed by NASA for vacuum conditions in outer space. Then the gold pads on the micro-sensor chip were connected to the TO-39 header using a MECH-EL 827 BALL BONDER from Mechel Corporation. The packaged micro-sensor is shown in Figure 2-6.

2.4 NOPF6 Doping

Micro-sensors coated with P3HT thin film were all doped using nitrosonium hexafluorophosphate (NOPF6)/acetonitrile solution to increase the conductivity. NOPF6/acetonitrile solution was purchased from Alfa-Aesar Company.

All doping was performed under air by soaking the micro-sensors (bare and packaged) in the doping solution and then the doped sensors were dried for at least 5 minutes. By varying the concentration of NOPF6/acetonitrile solution and the doping time, an optimum doping condition was established that yielded a final resistance of 1 to 10 ohms in the doped sensors.
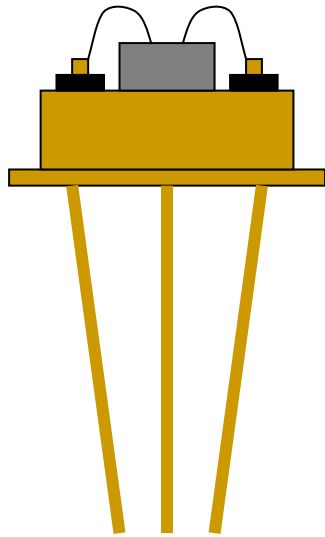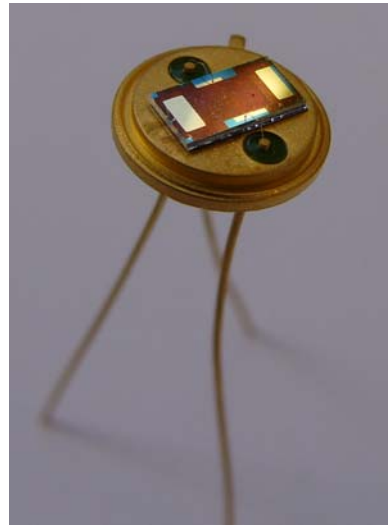
(a)   (b)
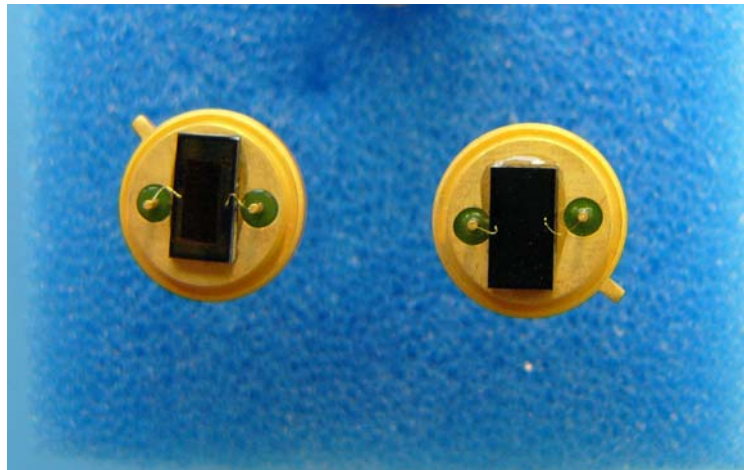
(c)

Figure 2-6   (a) Schematic of the TO-39 header, (b) The packaged P3HT thin film micro-sensor, and (c) The top view of packaged micro-sensor

2.5   Experimental Procedure for P3HT Thin Film Characterization

In the UV/visible, X-ray, and AFM studies, P3HT thin film were prepared by the spin coating method with a 200 nm thickness.   Some of the films were thermally annealed in an oven at different temperatures for 1 hour and some of them were kept in the no heat treatment state (control state) for comparison.

The optical absorption of P3HT films on glass slides in their undoped, NOPF6/acetonitrile doped, un-annealed (no heat treatment) and annealed states were measured using an UV/visible spectrophotometer (Ultospec 2100).   The spectra were taken over the wavelength range from 350 nm to 900 nm and 30 scans (scan speed: 30nm/sec) were used for all measurements.   The reference was a clean glass slide, and the UV spectrometer was referenced before each test to account for any drift in the spectrometer.   Following the progression of events in the sequence, UV/Visible Spectra of undoped P3HT films with about 200 nm thickness were first made by the spin coating technique at 3000 rpm and 30 seconds.   Next, UV/Visible Spectra were obtained of the films after doping them to the low resistance levels.   The optical absorption of P3HT films (~200nm) on glass slides in their un-annealed (no heat treatment) and annealed states were also measured using the same procedure.

X-ray diffraction measurements were performed with a Rigaku powder diffractometer in reflection geometry (θ-2θ scans).   The radiation was a monochromatized Cu K_α beam with wavelength $\lambda = 0.154$ nm. The X-ray studies were used to examine the structural properties and the type of crystalline order that prevails through the thickness of the no heat treatment and annealed films.

AFM measurements provided images of the top surface of P3HT films. Experiments were performed with a JSPM-5200 scanning probe microscope. The phase and height images were obtained simultaneously when operating the instrument in the tapping mode.

2.6 Experimental Procedure for Hydrazine/MMH Exposure Tests

2.6.1 Sample preparation

Packaged and bare $NOPF_6$ doped micro-sensors were prepared for high concentration level exposure tests. No heat treatment and annealed micro-sensors (doped bare sensors) were prepared for low concentration level exposure tests. The initial resistance of heavily and lightly doped sensors was between 1 Ω and 9 Ωs.

2.6.2 Hydrazine/MMH generation system

A model 491M precision gas standards generator with calibrated hydrazine permeation tubes, purchased from Kin-Tek Laboratories, was used to generate part-per-billion (ppb) to part-per-million (ppm) hydrazine/MMH streams diluted with nitrogen gas. This device works by mixing a small flow of component gas (hydrazine/MMH) to a larger flow of dilution gas (ultra-high purity, grade 5, nitrogen).

Hydrazine/MMH concentration in the gas mixture is determined by the equation provided by Kin-Tek Laboratories:

$$C = \frac{E \times Ko}{F \times 1000} \qquad (2\text{-}1)$$

Where,

E is the emission rate of component compound (hydrazine/MMH) from the

permeation tube in ng/min,

K_o is a constant converting the emission rate from a weight per minute to volume

per minute basis,

F is the dilution gas (nitrogen) flow rate in l/min at STP conditions, and

C is the hydrazine concentration in ppm ($\frac{\upsilon}{\upsilon}$).

Disposable tubes are supplied with the emission rate data usually in nanograms per minutes as listed in table 2-4. According to the equation, all of the tubes can be randomly combined or used separately to obtain the required gas concentration with the assistance of nitrogen flow rate adjustment. Before hydrazine/MMH exposure testing, each disposable tube was installed in the generator by using a glass adaptor bottle and then heated to the set temperature (80°C) for more than 4 hours to reach stabilization. The accuracy of gas concentration output is around $\pm$ 4% based upon calibration testing results from Kin-Tek Laboratories.

2.6.3 Hydrazine/MMH exposure system

The hydrazine/MMH exposure experimental set up was placed under a fume hood. The experimental exposure system is composed of the gas generator, sensor test fixture, waste gas absorption/reaction chamber, and data acquisition system. Figure 2-7 shows schematic diagrams of the hydrazine/MMH generation and exposure system set up for under different temperature exposure conditions. The gas streams were delivered to the closed test fixture via TetraFluorEthylene-Perfluorpropylene (FEP) Teflon tubing. The

test micro-sensor was installed inside the test fixture and placed near the gas inlet port to minimize potential interaction of hydrazine/MMH with other surfaces (see Figure 2-8). The increase in sensor resistance upon exposure to the hydrazine/MMH stream was recorded in real-time using an Agilent 34970A data acquisition system. The waste hydrazine/MMH stream was then delivered into a disposal chamber containing calcium hypochlorite, where the following reactions occurred:

$$Ca(ClO)_2 + N_2H_4 \rightarrow CaCl_2 + N_2 + H_2O \qquad\qquad (2\text{-}2)$$

$$Ca(ClO)_2 + CH_3NHNH_2 \rightarrow CaCl_2 + N_2 + CH_3OH + H_2O \quad (2\text{-}3)$$
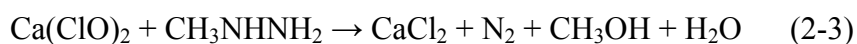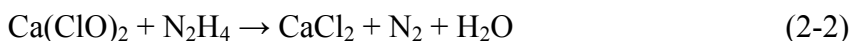
The room temperature hydrazine/MMH generation and exposure system was modified to perform the experiments at $70^{\circ}C$. A nitrogen gas bypass, a NESLAB temperature circulator/bath, and two heat exchange coils were added to the exposure system. The temperature bath (filled with distilled water) was used to reach exposure temperatures above room temperature by passing the gases through heat exchange coils submerged in the working fluid of the temperature bath. To make sure the temperature inside the test fixture reached the expected value ($70^{\circ}C$), a heating tape wrapped outside the test fixture was used to externally heat the test chamber and an Omega, K-type, thermocouple probe was installed inside the test fixture for temperature measurement. The Agilent 34970A data acquisition was connected to record the resistance and temperature data simultaneously. When the experiment started, the hydrazine/MMH stream was delivered through one of the coils to the test fixture while the nitrogen gas from the bypass line was delivered by another heated coil. When the temperature inside the test fixture hit $70^{\circ}C$, 25 ppm hydrazine/MMH was introduced into the test fixture.

Table 2-4   Emission rate of Hydrazine/MMH from individual permeation tube

Serial No	Permeating Fluid	K_0	Temperature ($^{\circ}$C)	Emission Rate (ng/min)
30072	Hydrazine	0.699	80	672
30074				1508
30077				2877
30078				2968
30079				2905
30080				2920
30081				2856
38481	MMH	0.487	80	5065
38659				5165
38660				5215

Vent

N$_2$

N$_2$ + N$_2$H$_4$

Sensor

N$_2$

Gas generator

Test fixture

Waste gas
disposal chamber

Data acquisition
system
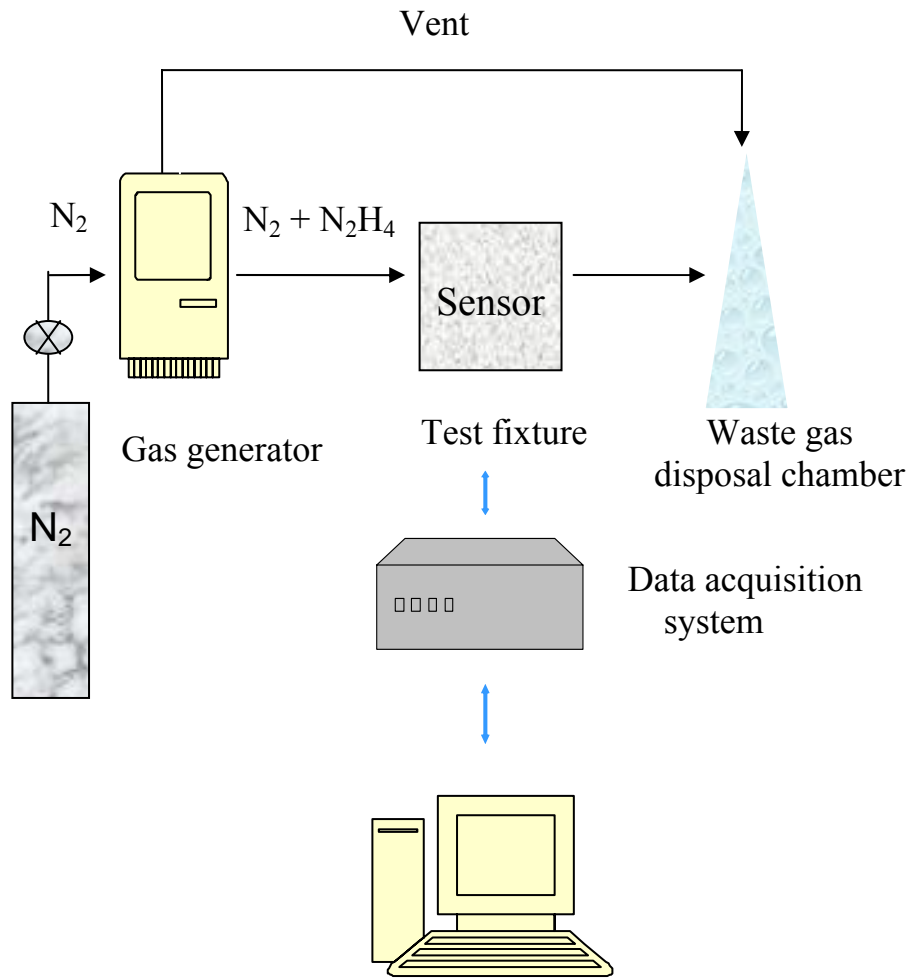
Fig 2-7   (a) Schematic diagram of Hydrazine/MMH generation and exposure system at
room temperature

Vent

Sensor

Gas generator

Test fixture

Waste gas
disposal chamber

N₂

Temperature bath

Data acquisition
system
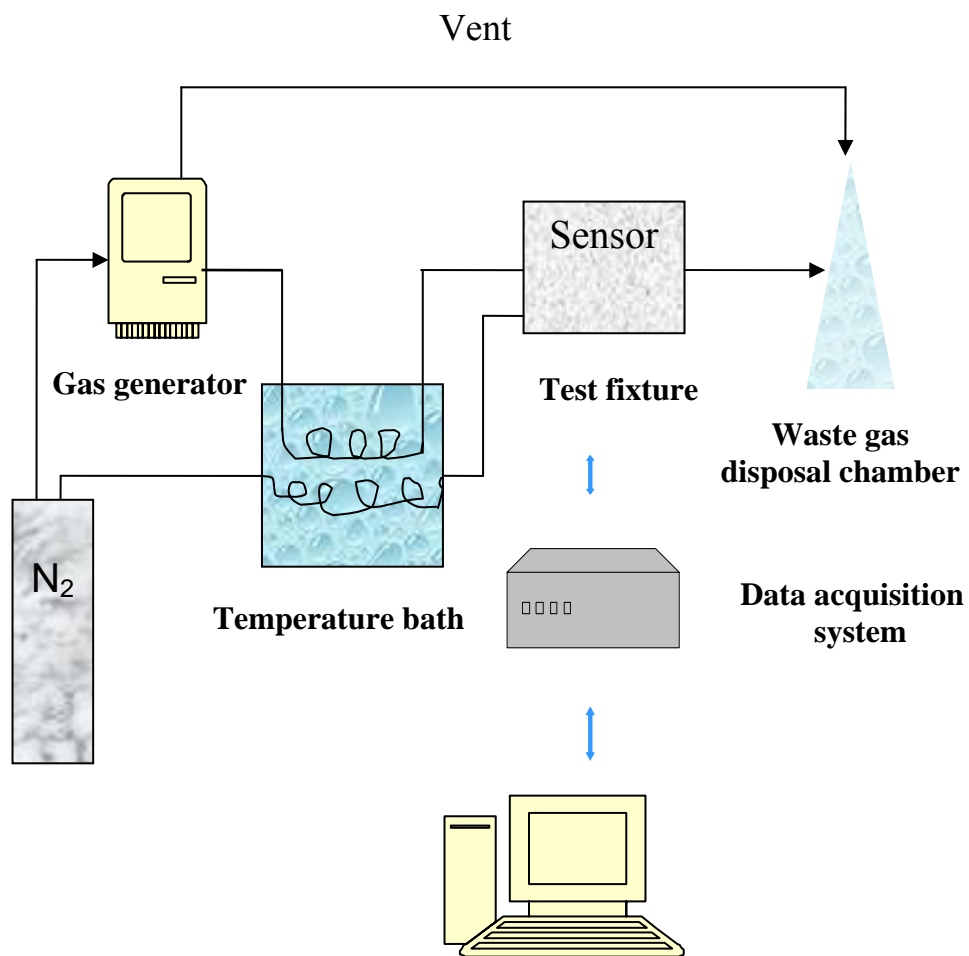
Fig 2-7   (b) Schematic diagram of Hydrazine/MMH generation and exposure system at high temperature

43

Display of flow rate and oven temperature

Oven temperature
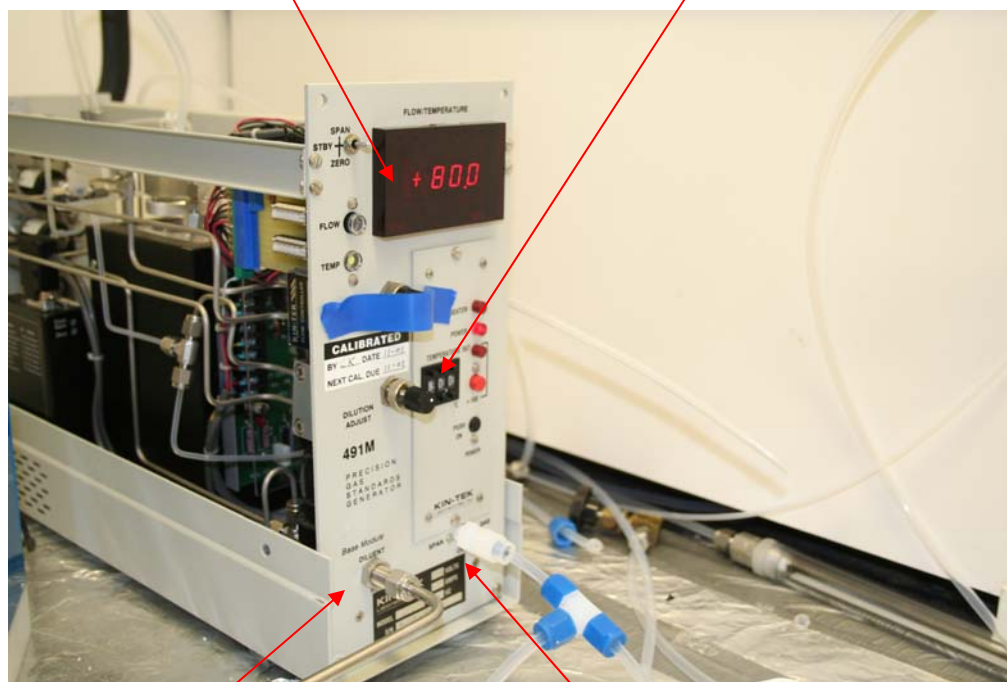
Nitrogen gas inlet

Hydrazine/MMH vapour outlet

Figure 2-8   (a) Kin-Tek 491M-BM gas standards generator

Gas inlet

Gas outlet

(b)

(c)

(d)

(e)
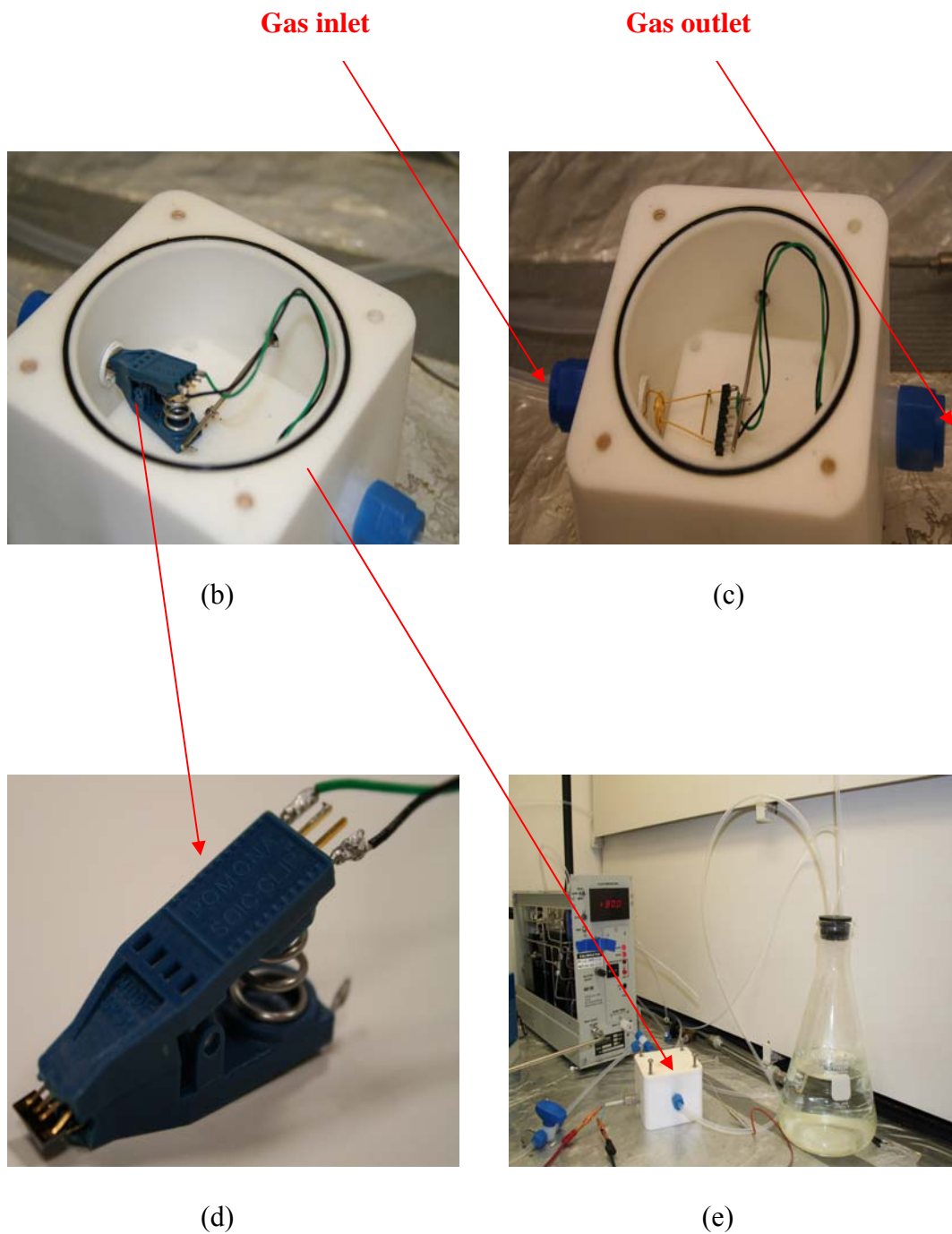
Figure 2-8   (b) Teflon test fixture with bare micro-sensor, (c) Teflon test fixture with packaged micro-sensor, (d) Connection of P3HT thin film micro-sensors for electrical measurement, and (e) Hydrazine generation and closed exposure system

2.7   Experimental Procedure for Stability Tests with P3HT Micro-sensor

2.7.1   Sample Preparation

Part of the P3HT thin film micro-sensor used in stability studies were the bare no heat treatment sensors while others were thermally annealed sensors.   The micro-fabricated sensor platforms were once again spin coated with a 200 nm P3HT thin film, and then were doped with different concentration levels of NOPF6/acetonitrile solution. The initial resistance of each heavily doped and lightly doped sensor was separately between 1 Ω and 9 Ω.

2.7.2   Experimental Procedures

The set up for sensor stability tests consisted of a Teflon test fixture, Data Acquisition System (Agilent 34401A), thermocouple, humidity sensor (honey well HIH-3602-C), and gravity convection oven (Lindberg /Blue).   The Agilent Benchlink data logger software was installed in the PC to record the resistance measurement data. Since the size of each micro-fabricated sensor is very small, it is not suitable to handle and measure the resistance of each sensor by hand using a digital multimeter and test leads. A special teflon-based test fixture was designed for continuous stability tests at room temperature and high temperature (see Figure 2-9). This test fixture has many advantages such as: (1) the position of each sensor is fixed so that resistance measurements are always made across the same region throughout a test; (2) the chance of scratching the P3HT polymer with the test leads of a general multimeter is eliminated; (3) up to 12 micro-sensors can be tested at the same time so that duplicate data are available for one
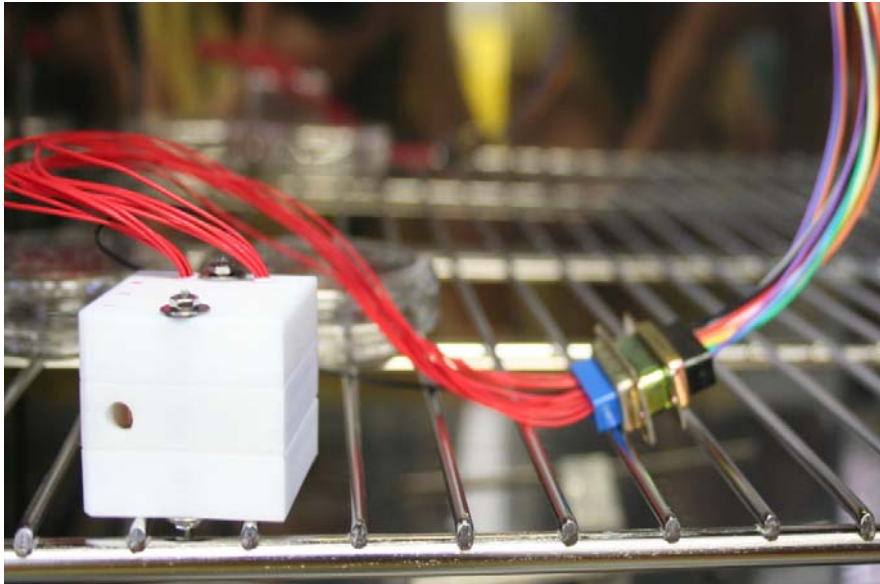
(a)
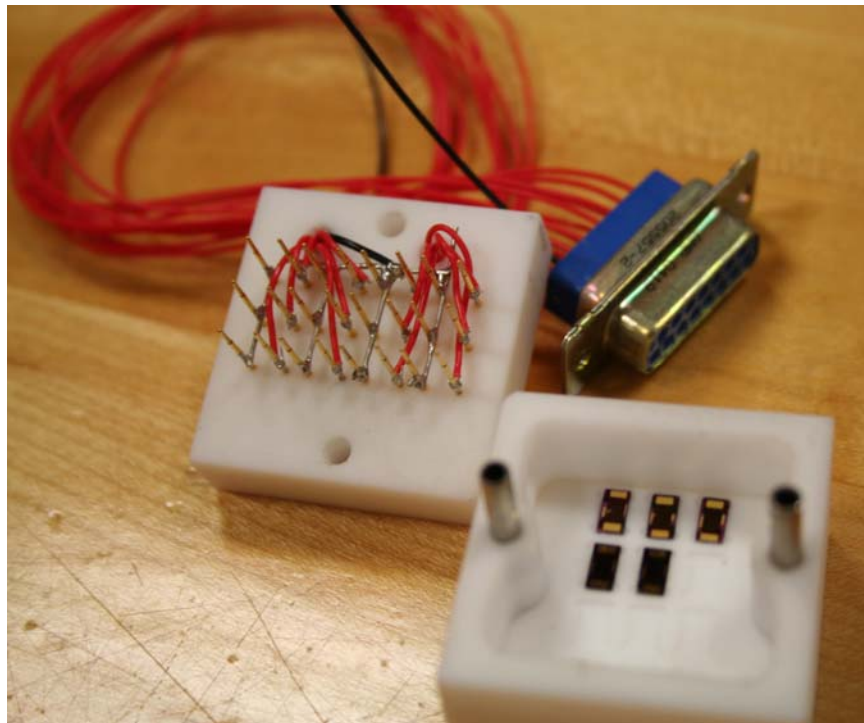
(b)

Figure 2-9   (a) Side view of whole teflon test fixture connected to the data acquisition system, and (b) Top view of the inner design of test fixture

set of test conditions; and (4) continuous measurements can be performed to record

consistent and accurate data. For the stability tests at the high oven and the humidity

sensor is used to record the relative humidity of the outside environment. Figure 2-10

shows the experimental set up for the stability tests at the high temperature.

Figure 2-10   Front view of experimental set up for micro-sensor's stability test at 70°C

CHAPTER 3

RESULTS AND DISCUSSION: CHARACTERIZATION OF

POLY (3-HEXYLTHIOPHENE) THIN FILM

Head-to tail coupled P3HT is one of the most promising materials that combines straight forward processability with high charge carrier mobility. Although the electronic transport mechanism inside the P3HT film is not well understood due to its complex heterogeneous structure, the fact that orientation and structural order can affect the electronic properties has been established [38]. This chapter presents the results of Ultraviolet-visible absorption spectroscopy, X-ray, and Atomic Force Microscopy characterizations of Poly (3-Hexylthiophene) thin film processed using different methods. The structural properties of undoped and doped; no heat treatment and annealed P3HT thin films are explored and discussed.

3.1   UV/Visible Spectra of Poly (3-hexylthiophene) Thin Film

Fig 3-1 shows a typical UV/Visible Spectrum for undoped and doped P3HT thin films. The undoped P3HT thin film is initially orange in color, and its characteristic spectrum is a broad peak at 516 nm corresponding to the π - π^* transition in conjugated polymer, which indicates the transition between energy levels of the π electronic system. The doped P3HT thin film is light blue in color, and its spectrum showed a second broad peak at 750 nm corresponding to bipolaron absorption. This peak was less intense than the π - π^* peak. As mentioned in the previous section, biopolarons are believed to be the source of charge carriers in the doped (oxidized) conducting polymer [15]. UV/Visible spectrum data indicated the doping (oxidation) process of P3HT film results in a large increase of charge carriers in the films.

Figure 3-2 represents the effect of thermal annealing on the UV-Vis absorption spectra for the P3HT thin films spun coated on glass substrates. The annealing time for all temperatures was 1 hour. As the annealing temperature was increased, the absorption spectra at both 530 and 600 nm increased. Increased interchain interaction is the key factor that is thought to increase the absorption at these wavelengths. These changes further indicate an increasing degree of ordering of the polymer chains in the film.
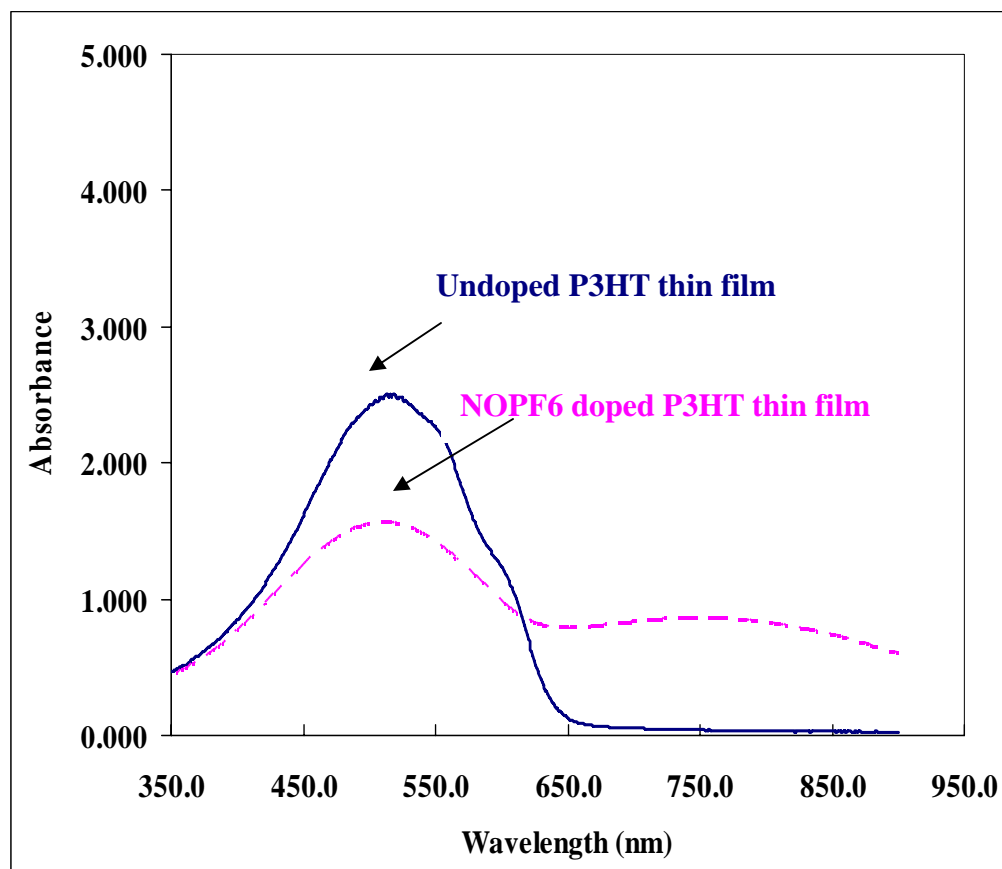
Fig 3-1   UV/visible spectrum of undoped and NOPF6 doped P3HT thin films
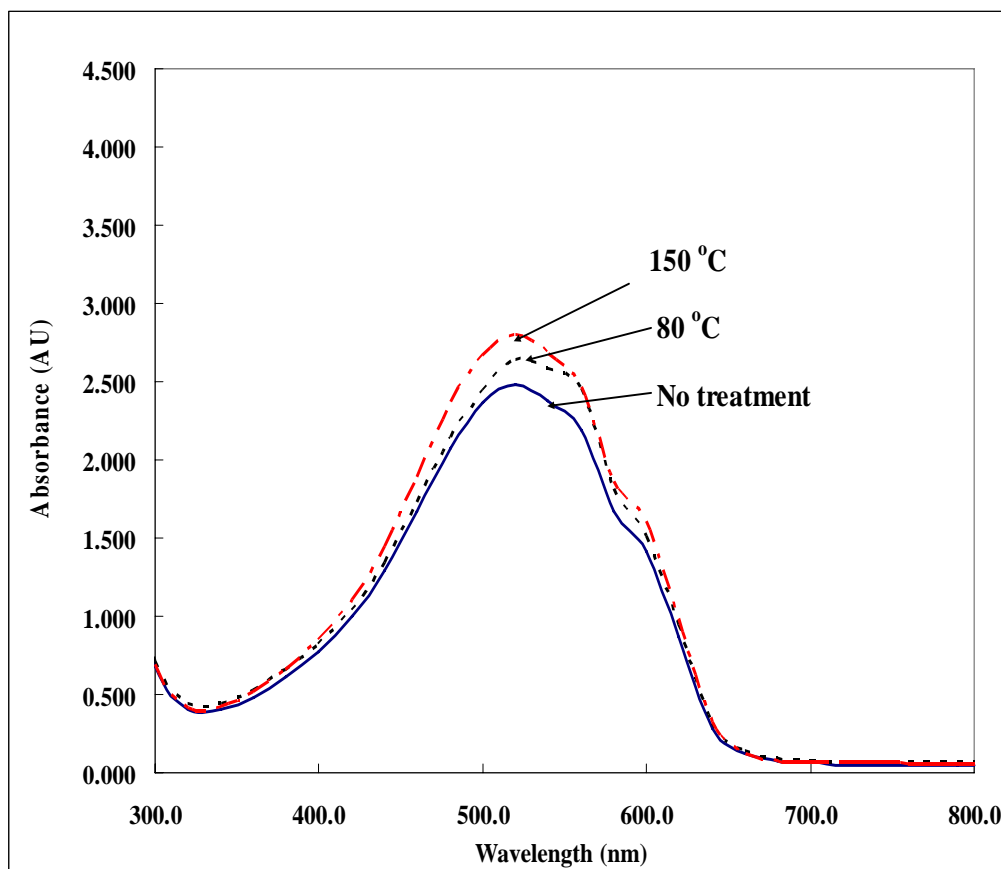
Figure 3-2   Absorption Spectra for P3HT thin films before and after annealing at different temperatures for 1 hour

3.2   XRD Analysis and AFM Imaging of Poly (3-hexylthiophene) Thin Film

XRD and AFM measurements were used to investigate the morphological changes

in the polymer layer as a result of thermal treatment. The X-Ray diffraction pattern of

P3HT thin film before and after annealing is shown for angles between 3 and 10 degrees

2θ in Figure 3-3.   After thermal annealing, the single peak observed at $2\theta = 5.4^o$ moves

towards lower angles ($2\theta = 5.2^o$) and becomes much sharper. The size of the polymer

crystallites L can be estimated by the Scherrer formula

$$L = \frac{0.9\,\lambda}{\text{B} \cos \theta} \qquad\qquad (3\text{-}1)$$

where λ is the radiation wavelength (0.154 nm) and B is full width half maximum

of the peak. According to the equation, the crystallite size of the no treatment and

annealed P3HT thin films was 0.11 nm and 0.23 nm respectively.   The increased

crystallite size of P3HT film suggests that the conjugation length of P3HT has increased

during the thermal annealing process. According to the theory, polythiophenes have

relatively low rotational barriers. This makes the chains very flexible and increases the

possibility of twisting along the backbone. The rotation of the P3HT chain can decrease

the conjugation length, increase the band gap, and finally reduce the conductivity of the
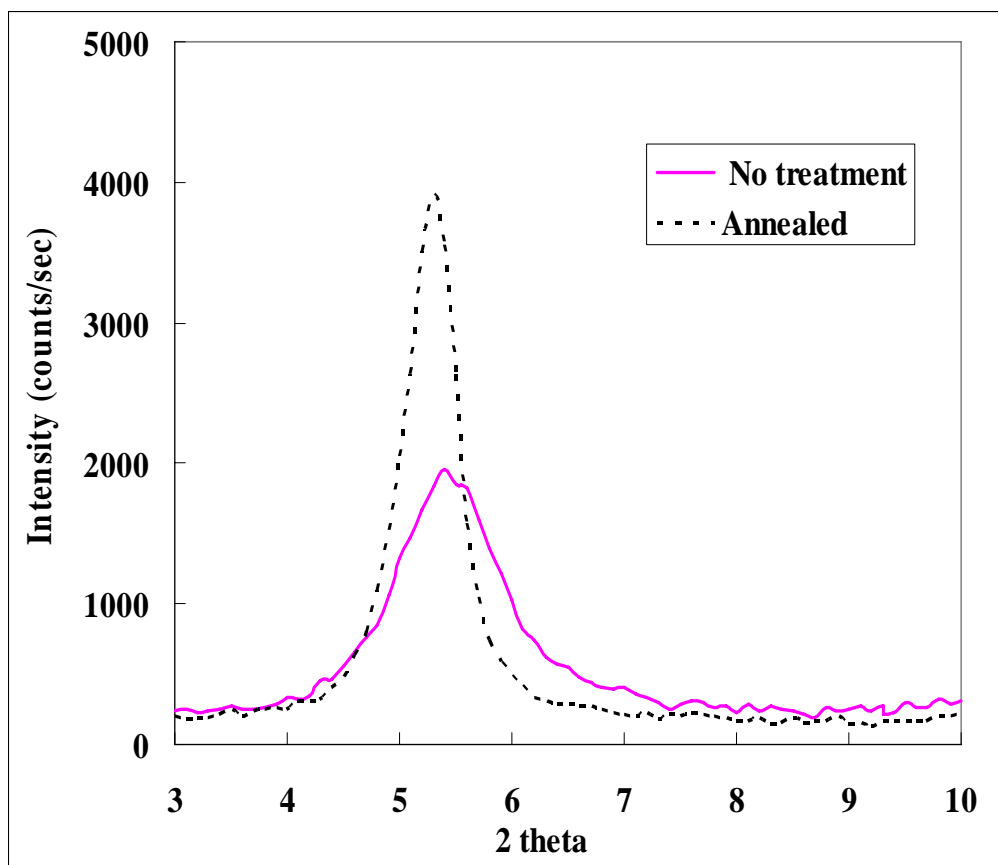
Figure 3-3　X-ray diffraction spectra of pre-annealed and 190°C-1 hour thermally annealed P3HT thin films

film [39]. Therefore, the increased crystallite size of P3HT thin film results in an improvement of the thermal stability of the film.

The AFM image in Figure 3-4 shows the active layer surfaces of no treatment and annealed films. The films that were thermally treated at 190°C for 1 hour had larger average surface roughness (Ra = 3.44 nm) than the no treatment film (Ra = 1.71 nm). This change corresponds to an increased density of the organic film, an enhancement of intermolecular interaction which leads to better device performance, and also a decreased concentration of defects by evaporation of the solvent and water.
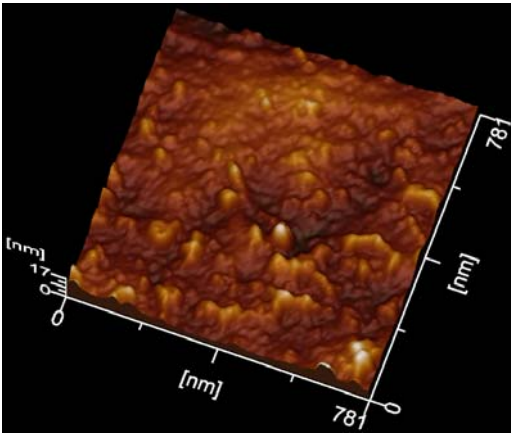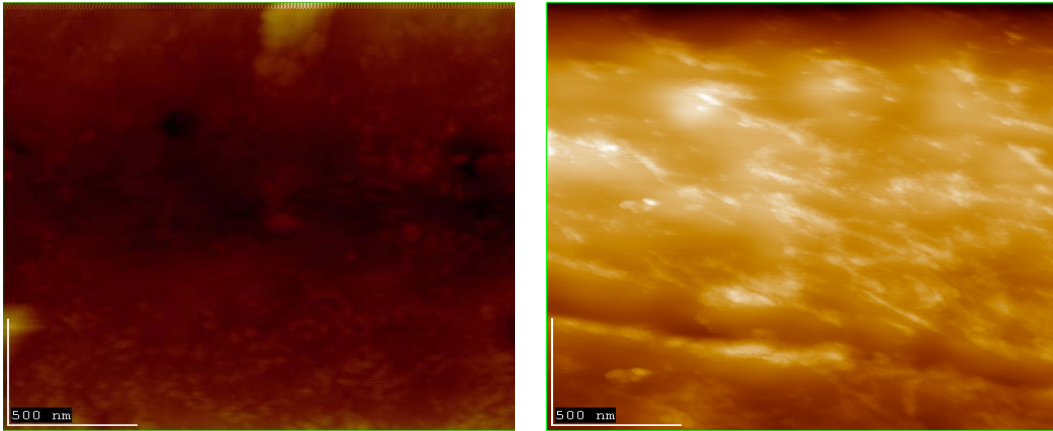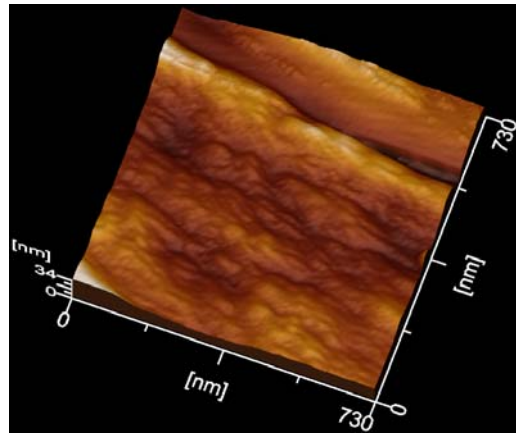
(a) No heat treatment   (b) 190°C for 1 hour

Figure 3-4   AFM phase images of P3HT thin films by spin coating before and after annealing (a) before annealing, Ra = 1.71 nm and after annealing at (b) 190°C for 1 hour, Ra = 3.44 nm

CHAPTER 4

RESULTS AND DISCUSSION: HYDRAZINE/MMH RESPONSE

The potential use of Poly (3-hexylthiophene) (P3HT) as the sensing element for hydrazine/MMH vapor detection will be presented in this chapter. Exposure of NOPF6 doped, P3HT thin film, micro-sensor to hydrazine/MMH vapor results in an irreversible and easily monitored increase in the electrical resistance of P3HT thin film. The effects of vapor concentration, temperature and thermal treatment on the sensor's resistance are described in this chapter.

4.1 Control Experiments

The first experiment was performed to study the sensor's baseline response to nitrogen gas. Six NOPF6 doped sensors were sequentially exposed to flowing nitrogen gas at a fairly high flow rate (4 l/min) for 30 minutes. The average response curve of 6 sensors, shown in Figure 4-1, indicates that the doped P3HT thin films do not respond
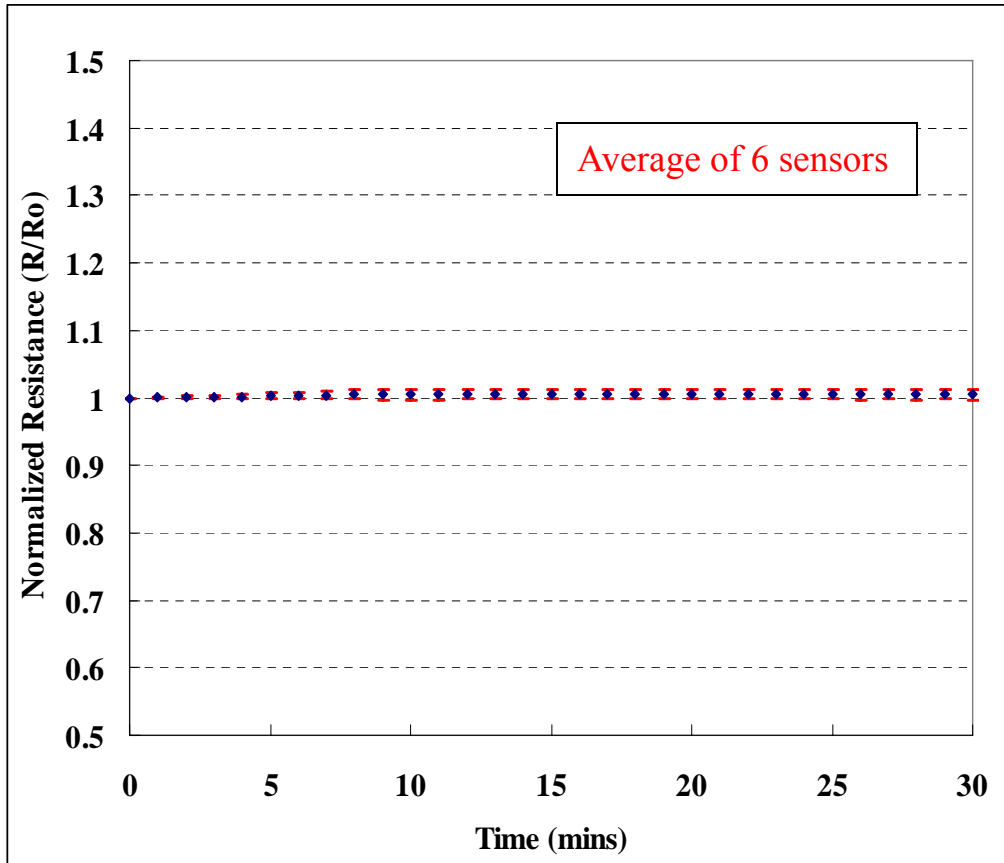
Figure 4-1   Response of P3HT thin film micro-sensor to a 4 l/min N_2 stream at $25^{\circ}C$

(are not sensitive) to flowing nitrogen gas. The very slight change in resistance may be due to the removal of a small quantity of absorbed water vapor in the P3HT films.

4.2   Response of Bare P3HT Micro-sensors to Hydrazine/MMH at 25 ppm

In this study, nitrogen gas was used to deliver and dilute hydrazine/MMH gas in the generation and exposure system. All data are presented in units of resistance (R). Since the starting resistance of each sensor was not always the same, the data are normalized to the initial resistance (Ro), and the data from all the hydrazine/MMH exposure experiments are presented as normalized resistance (R/Ro) versus time (minutes). Table 4-1 lists all the parameters of hydrazine/MMH tests at 25ppm.

4.2.1   Hydrazine/MMH response at room temperature

Next, the response of the P3HT thin film micro-sensor to hydrazine/MMH vapor at room temperature was studied. A typical hydrazine response curve is shown in Figure 4-2. This response corresponds to the exposure of a 200 nm P3HT film-based micro-sensor to a 25 ppm hydrazine vapor (flow rate 0.4 l/min at 1 atmosphere pressure) introduced about 30 minutes into the experiment. The sensor was heavily doped to an

initial resistance of 1.5 Ω using a higher dopant concentration in the doping solution.

From the curve, the resistance of the P3HT thin film micro-sensor increases very rapidly within the first few seconds when immediately exposed to hydrazine. The normalized resistance of the sensor increased more than 7 orders of magnitude within 10 minutes. However, this response is not linear. The resistance increases more gradually with increasing exposure time. This decrease in the derivative of normalized resistance with respect to time as a function of increasing exposure time indicates a decline in the sensitivity of the film. This decrease in the sensitivity continues to occur until finally the sensor reaches a saturated state.

Monomethylhydrazine (MMH) is one of the hydrazine derivatives. The detection of MMH at low concentration levels is also very important to insure personnel safety. Figure 4-3 shows the sensor's response to exposure to 25 ppm MMH vapor in air at 0.3 l/min flow rate. This curve is very similar to the hydrazine curve at room temperature. The sensor shows a sharp increase in resistance within several minutes and then saturation at high levels of MMH dose.

4.2.2 Hydrazine/MMH response at high temperature

Since the environmental temperature may change from -50°C to 70°C, it is necessary to investigate the response of the P3HT thin film micro-sensor to hydrazine/MMH vapor at different temperatures. Here we report the hydrazine/MMH response at 70°C.

Figure 4-4 and Figure 4-5 separately represents the result of real-time monitoring of 25 ppm hydrazine and MMH vapor in air at 70°C. The results show that at high temperature, the P3HT thin film micro-sensor is also capable of sensing hydrazine/MMH vapor within short time reaching orders of magnitude change in resistance.

According to the Arrhenius relationship the temperature dependence should be dependent upon activation energy following the form:

$$K = A \exp\left(\frac{-Q}{RT}\right) \qquad (4\text{-}1)$$

Where,

K is the normalized resistance increasing rate at certain temperature,

Q is the activation energy,

T is the absolute temperature,

R is the ideal gas constant, and

A is a constant.

when the temperature increases, the normalized resistance rate increases. This can be

seen in the Figure 4-4 and 4-5.
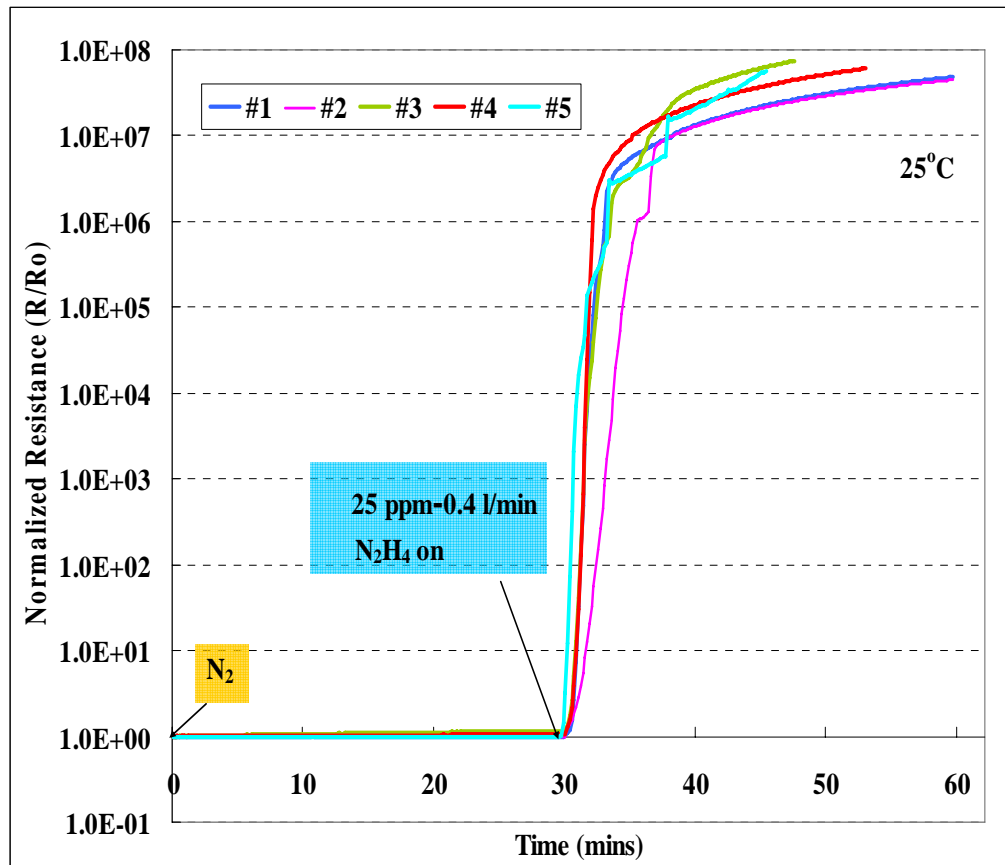
Figure 4-2   Sensor's dynamic response to 25 ppm, 0.4 l/min hydrazine stream at ambient pressure, 25°C
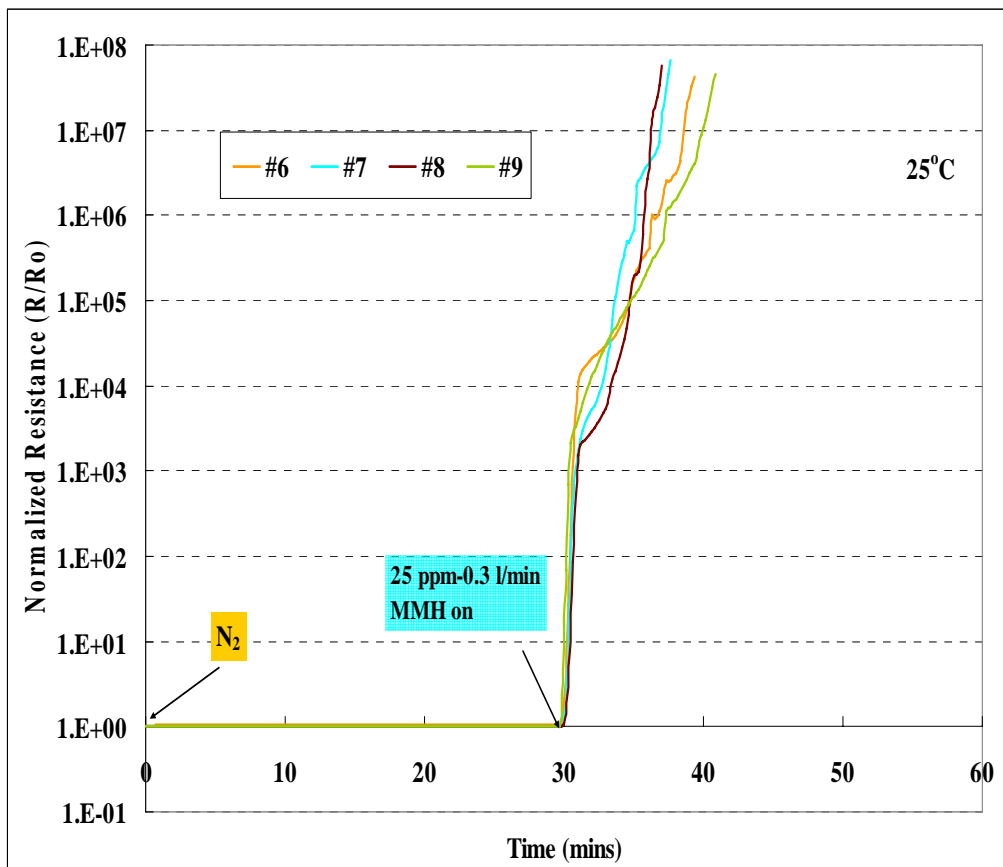
Figure 4-3   Real-time response of P3HT thin film micro-sensor to 25 ppm, 0.3 l/min MMH in air, at ambient pressure, 25°C
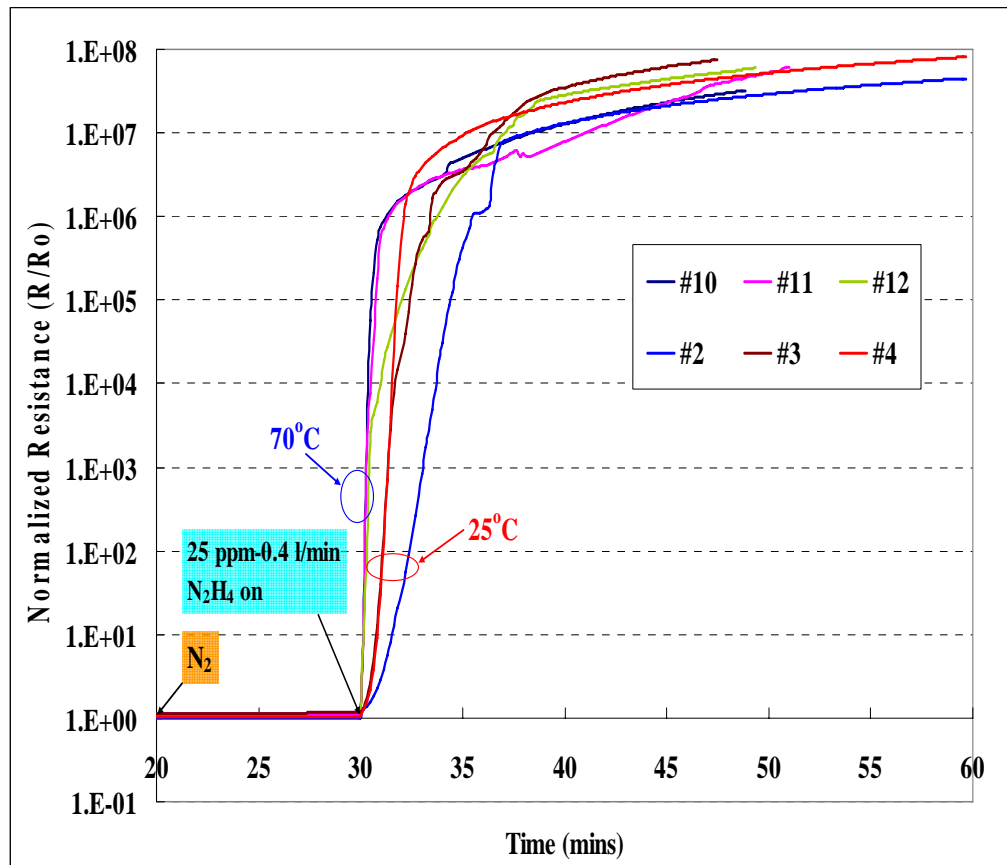
Figure 4-4   Real-time response of P3HT thin film micro-sensor to 25 ppm, 0.4 l/min hydrazine in air, at ambient pressure, $70^{o}C$
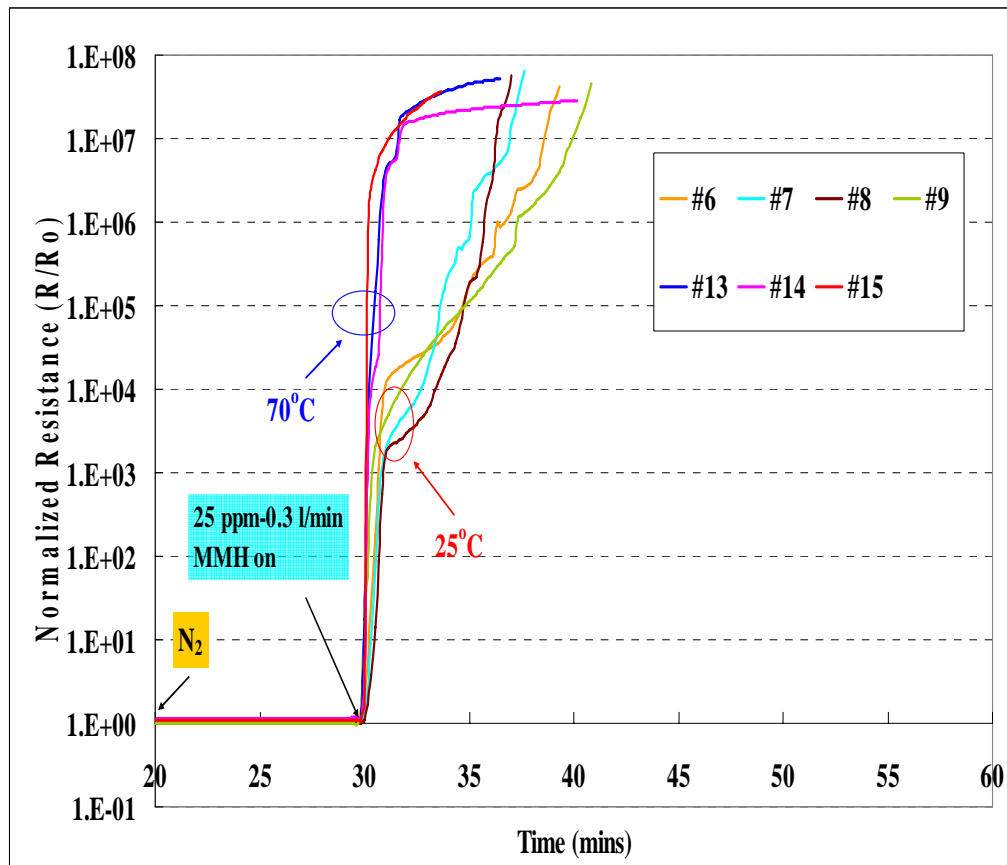
Figure 4-5   Real-time response of P3HT thin film micro-sensor to 25 ppm, 0.3 l/min MMH in air, at ambient pressure, $70^{\circ}C$

Table 4-1   Test Parameters for Hydrazine/MMH response tests at 25 ppm

Sample	Gas	Temperature	Flow rate	Ro
#1	N_2H_4	25^oC	0.4 l/min	1.51
#2	N_2H_4	25^oC	0.4 l/min	1.41
#3	N_2H_4	25^oC	0.4 l/min	1.48
#4	N_2H_4	25^oC	0.4 l/min	1.45
#5	N_2H_4	25^oC	0.4 l/min	1.50
#6	MMH	25^oC	0.3 l/min	1.58
#7	MMH	25^oC	0.3 l/min	1.56
#8	MMH	25^oC	0.3 l/min	1.60
#9	MMH	25^oC	0.3 l/min	1.52
#10	N_2H_4	70^oC	0.4 l/min	1.54
#11	N_2H_4	70^oC	0.4 l/min	1.42
#12	N_2H_4	70^oC	0.4 l/min	1.57
#13	MMH	70^oC	0.3 l/min	1.51
#14	MMH	70^oC	0.3 l/min	1.56
#15	MMH	70^oC	0.3 l/min	1.46

4.3   Response of Bare P3HT Micro-sensors to Hydrazine at ppb levels

4.3.1   Hydrazine concentration effects

Since the threshold limit value (TLV) of hydrazine has been lowered to 10 ppb for an 8 hour period, accurate and fast sensing of part-per-billion (ppb) levels of hydrazine in ambient environments is very necessary to insure personal safety.   In this study, hydrazine exposures of 518 ppb at 4 l/min, 263 ppb at 4 l/min, 117 ppb at 4 l/min, and 52 ppb at 9 l/min were generated by changing the nitrogen gas flow speed and hydrazine emission rate described in section 2.6.2.   Figure 4-6 shows the response of the P3HT micro-sensors to these concentration levels at ambient pressure and room temperature over the first 30 minutes.   Due to the limits of the hydrazine permeation tubes, the flow rate at concentrations of 52 ppb could not be set the same as the other concentrations at 4 l/min.   It can be seen that the response rate of the P3HT micro-sensor increased with increasing hydrazine concentration.   For the higher concentration levels,   the sensors were capable of responding to the hydrazine stream in less than a few minutes reaching several orders of magnitude change in normalized resistance.
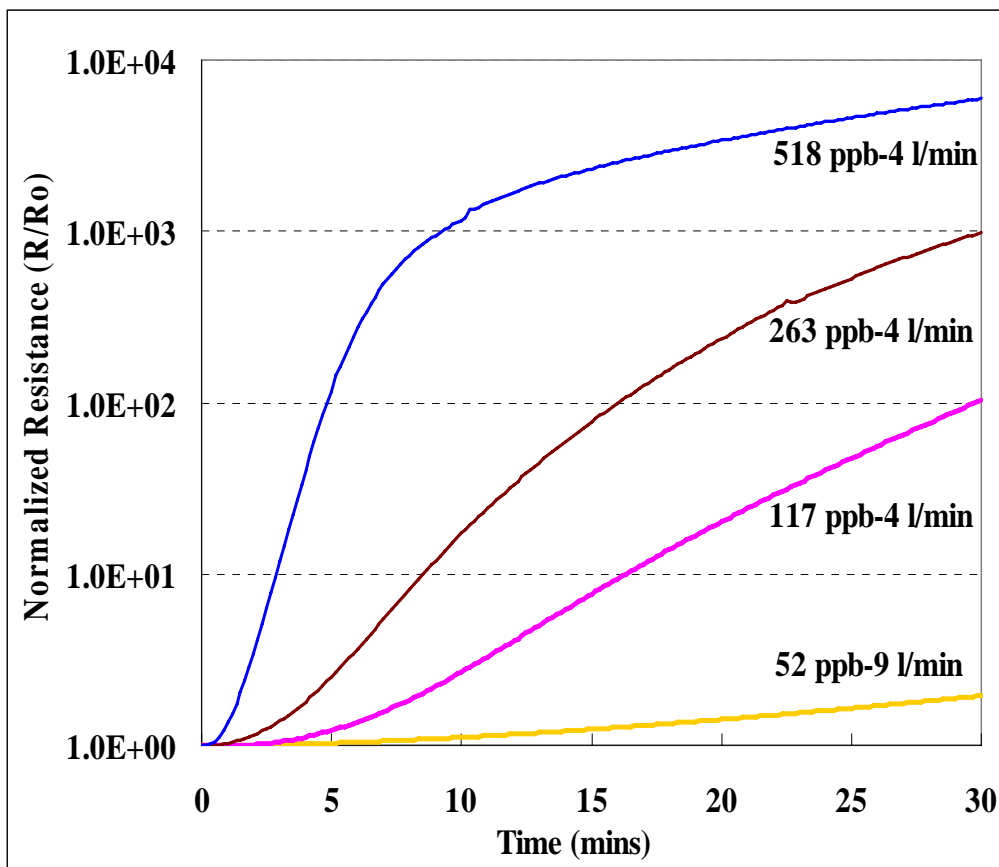
Figure 4-6: Real time response of P3HT micro-sensors to different hydrazine concentration at ambient pressure, $25^{o}C$

4.3.2 Doping level effect

In addition, different levels of doping also affect the sensing response of the P3HT thin film micro-sensors at ppb concentration levels. Although it is possible to dope the polymer to a higher conductivity (lower resistance) such as 1~1.5 Ω, which is better for stability as will be discussed in the next chapter, it was found that the sensitivity of the sensor to hydrazine at low concentration levels decreased when the sensor was heavily doped to lower initial resistances (see Figure 4-7).

4.3.3 Thermal annealing effect

Hydrazine exposure tests at low concentration levels were also performed at room temperature with annealed and pre-annealed sensors (see Figure 4-8). The results show that annealed P3HT thin film micro-sensors had better sensitivity to the hydrazine vapor at low concentration levels (i.e. 52 ppb) than the no treatment sensors. The performance of the device such as sensitivity can be improved by thermal annealing methods. Table 4-2 lists all the parameters of hydrazine response at 52 ppb concentration levels.
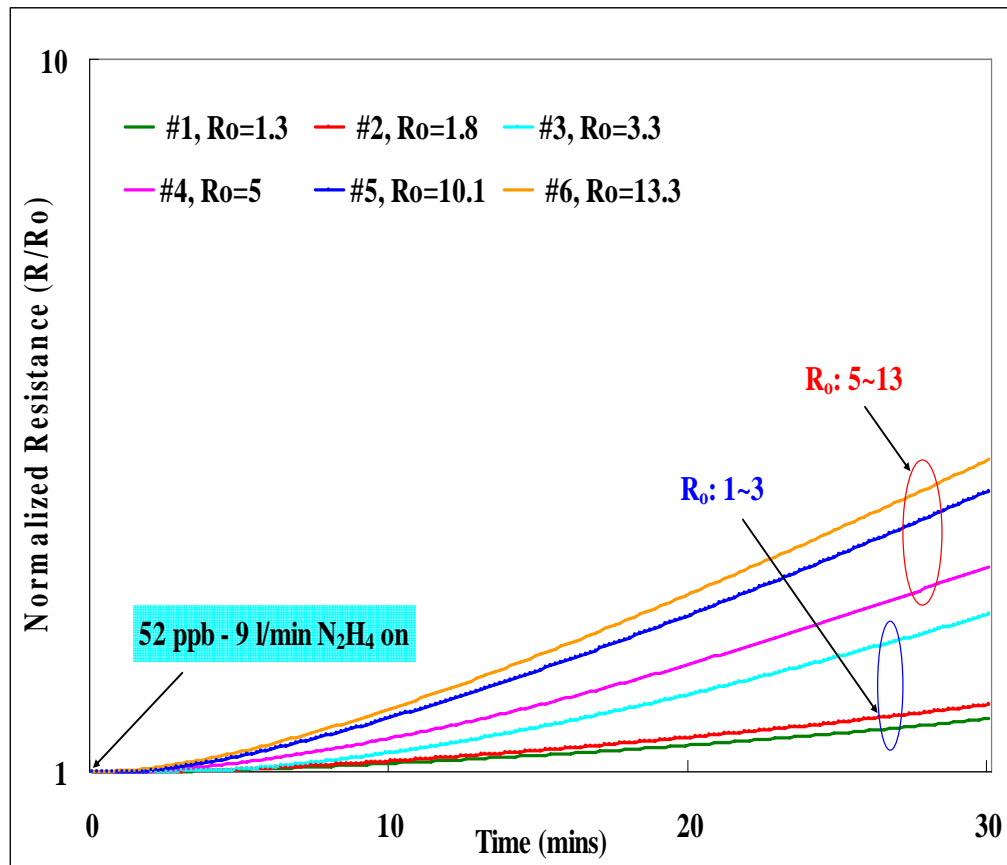
Figure 4-7   Response of P3HT thin film micro-sensors to hydrazine vapor at 52 ppb-9 l/min, ambient pressure, $25^{\circ}C$. Sensors were separately doped to different initial resistance levels.
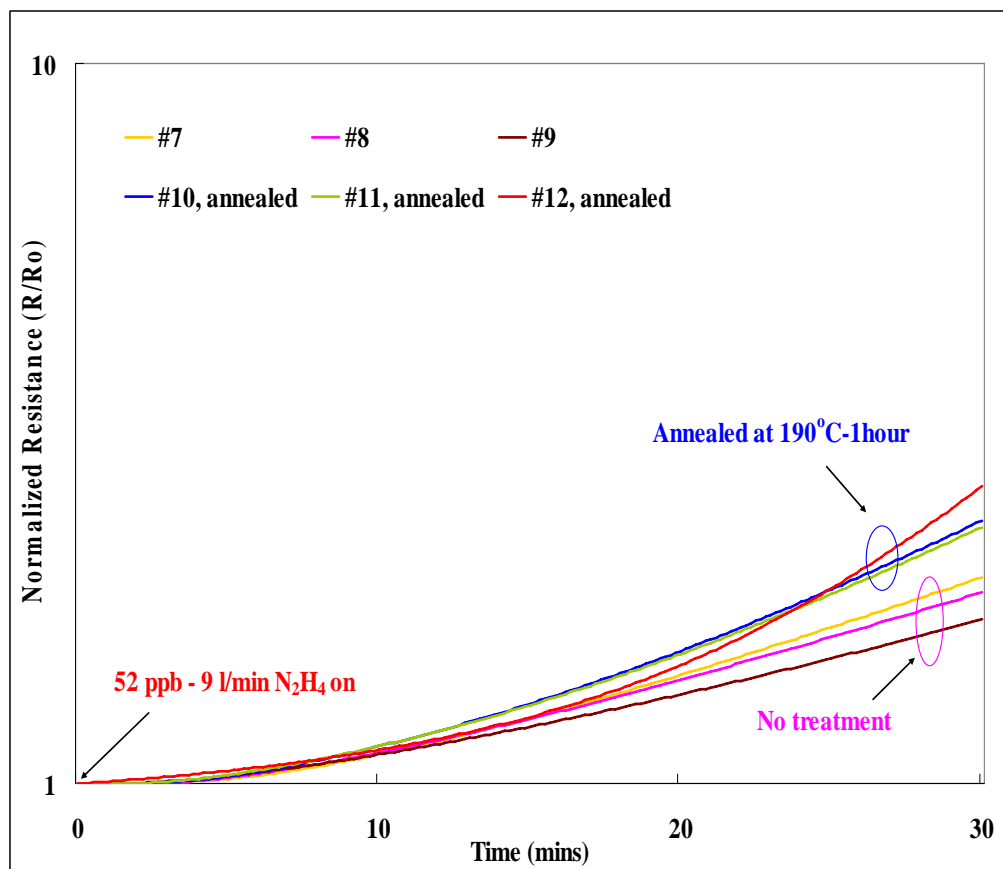
Figure 4-8   Real time response of annealed (190°C-1h) and no treatment P3HT micro-sensors to 52 ppb-9 l/min hydrazine gas at ambient pressure, $25^{o}C$

Table 4-2   Test parameters of Hydrazine response tests at levels, 25°C

Sample	Treatment	Concentration	Flow rate	R_o
#1	no treatment	52 ppb	9 l/min	1.3
#2	no treatment	52 ppb	9 l/min	1.8
#3	no treatment	52 ppb	9 l/min	3.3
#4	no treatment	52 ppb	9 l/min	5
#5	no treatment	52 ppb	9 l/min	10.1
#6	no treatment	52 ppb	9 l/min	13.3
#7	no treatment	52 ppb	9 l/min	12.2
#8	no treatment	52 ppb	9 l/min	13.1
#9	no treatment	52 ppb	9 l/min	11.6
#10	annealed	52 ppb	9 l/min	12.4
#11	annealed	52 ppb	9 l/min	12.8
#12	annealed	52ppb	9 l/min	11.9

4.4   Response of Packaged P3HT Micro-sensors to Hydrazine at 25ppm

The response of packaged P3HT micro-sensors to hydrazine vapor at 25 ppm-0.4

l/min was also investigated at room temperature. From Figure 4-9, it is obvious that

packaged sensors have a lower resistance change than bare sensors (see Figure 4-2). This

may be caused by the position of the packaged sensor inside the test fixture. Since the

size of packaged sensor did not allow the sensor to be inserted into the hydrazine gas inlet

to the same position as the bare sensor, it cannot be guaranteed that both sensors were

exposed to the same hydrazine concentrations. Hydrazine interacts with surfaces quickly

and the location of the packaged sensor may have significantly changed the concentration

of hydrazine that the sensor was exposed to. Table 4-3 lists the test parameters of these

exposure tests.

4.5   Sensor's Specificity

Another issue for this P3HT thin film micro-sensor is its specificity to hydrazine

vapor. Since hydrazine is a hypergolic compound that when combined with mixed

oxides of nitrogen self ignites, it is very necessary for this sensor to not react to mixed

oxides of nitrogen such as N_2O and NO_2. Figure 4-10 shows the response of the P3HT

thin film micro-sensor to high concentration levels of N_2O and NO_2 vapors. It is obvious that this sensor does not respond to N_2O and NO_2 at 100 ppm concentrations. This indicates the good specificity of this micro-sensor.
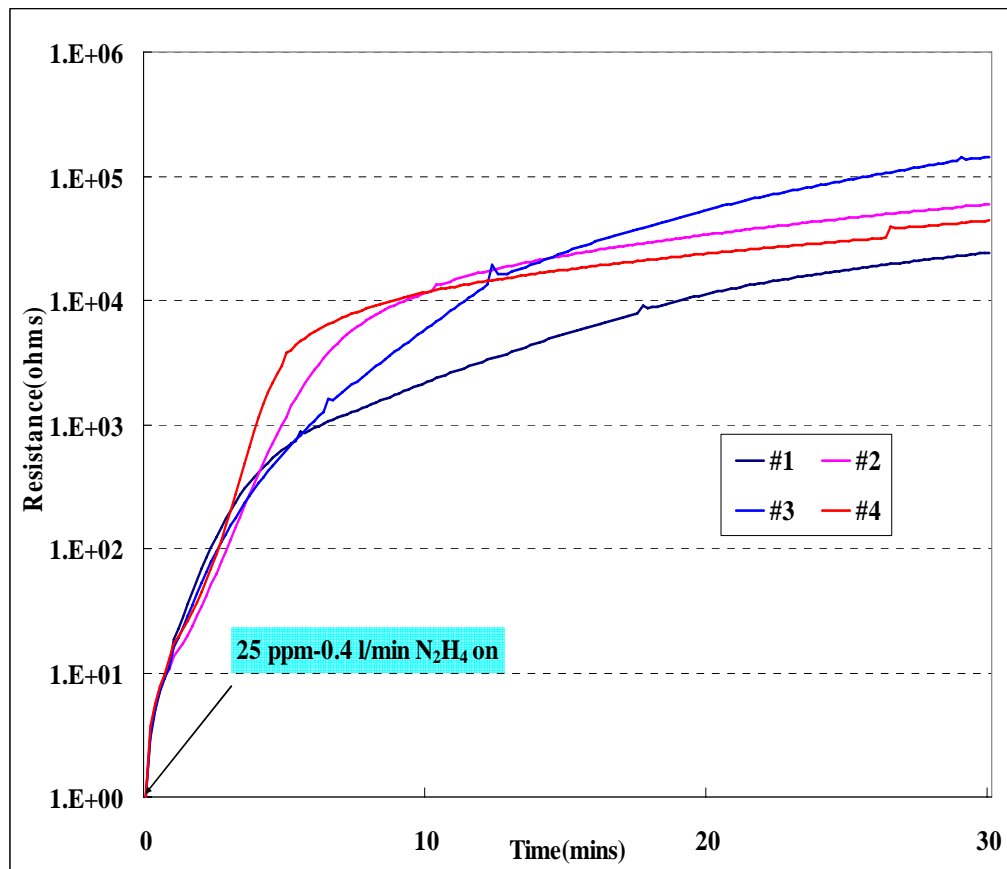
Figure 4-9   Packaged sensors' response to 25 ppm, 0.4 l/min hydrazine stream at ambient pressure, 25°C
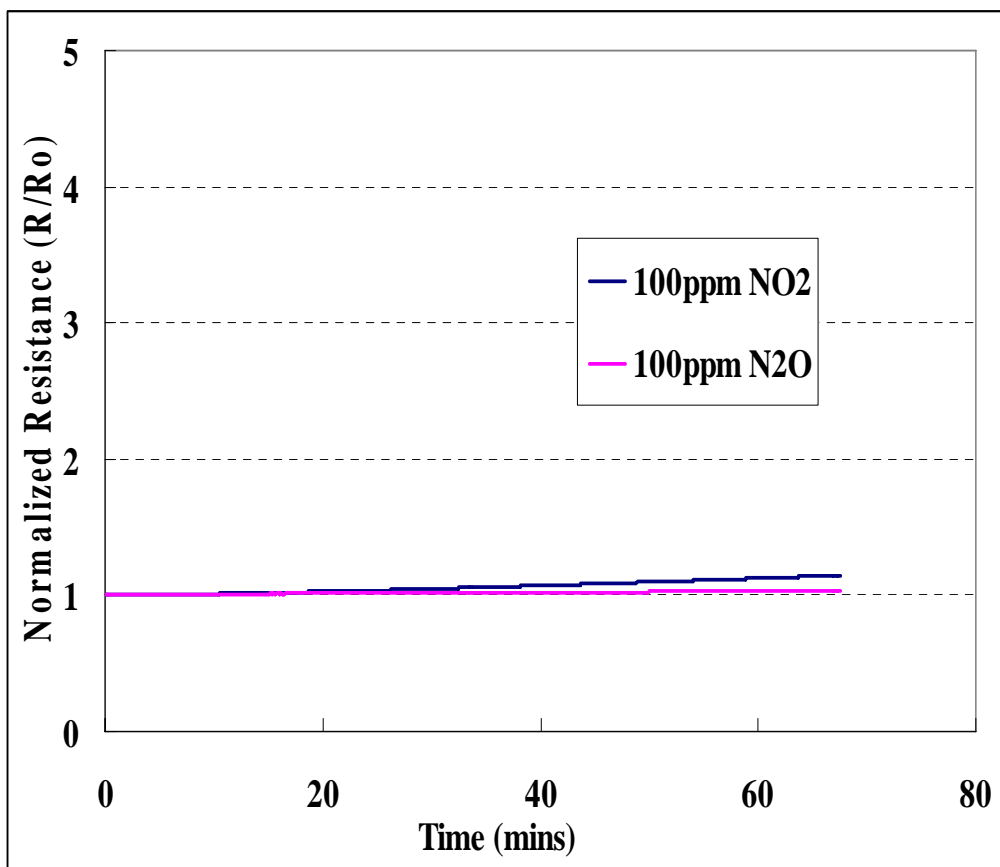
Figure 4-10   Response of P3HT thin film micro-sensors to NO_2 and N_2O vapor at 100 ppm, 1 l/min, 25°C

Table 4-3   Test Parameters of Hydrazine response tests with packaged sensors

Sample	Temperature	Concentration	Flow rate	R_o
#1	25^oC	25 ppm	0.4 l/min	1.53
#2	25^oC	25 ppm	0.4 l/min	1.46
#3	25^oC	25 ppm	0.4 l/min	1.51
#4	25^oC	25 ppm	0.4 l/min	1.52

CHAPTER 5

RESULTS AND DISCUSSION: STABILITY

This chapter explores the impacts of doping level and different thermal annealing temperatures on the stability of P3HT, thin-film-based, chemiresistor micro-sensor under different temperature conditions.

5.1   Stability Test of No Heat Treatment Micro-sensors

Figure 5-1 shows the resistance change of P3HT sensors doped by NOPF6/acetonitrile with different doping concentrations as a function of time at $25^{o}C$.   It can be seen that sensors doped by using a high concentration doping solution (0.5 g/ml) had less resistance change after 29 days than lightly doped sensors with 0.35 g/ml doping concentration.

The same case also occurred for stability tests conducted at high temperature as shown in Figure 5-2. It can be seen that the normalized resistance of sensors at $71^{o}C$ increased very quickly. The decay of conductivity follows the Arrhenius law. It has been proposed that a conformational change in the polymer backbone reduced the charge carriers in the doped polymer and caused the regeneration of the doped polymer at higher temperatures [38]. The normalized resistance of sensors at $25^{o}C$ had a lower resistance
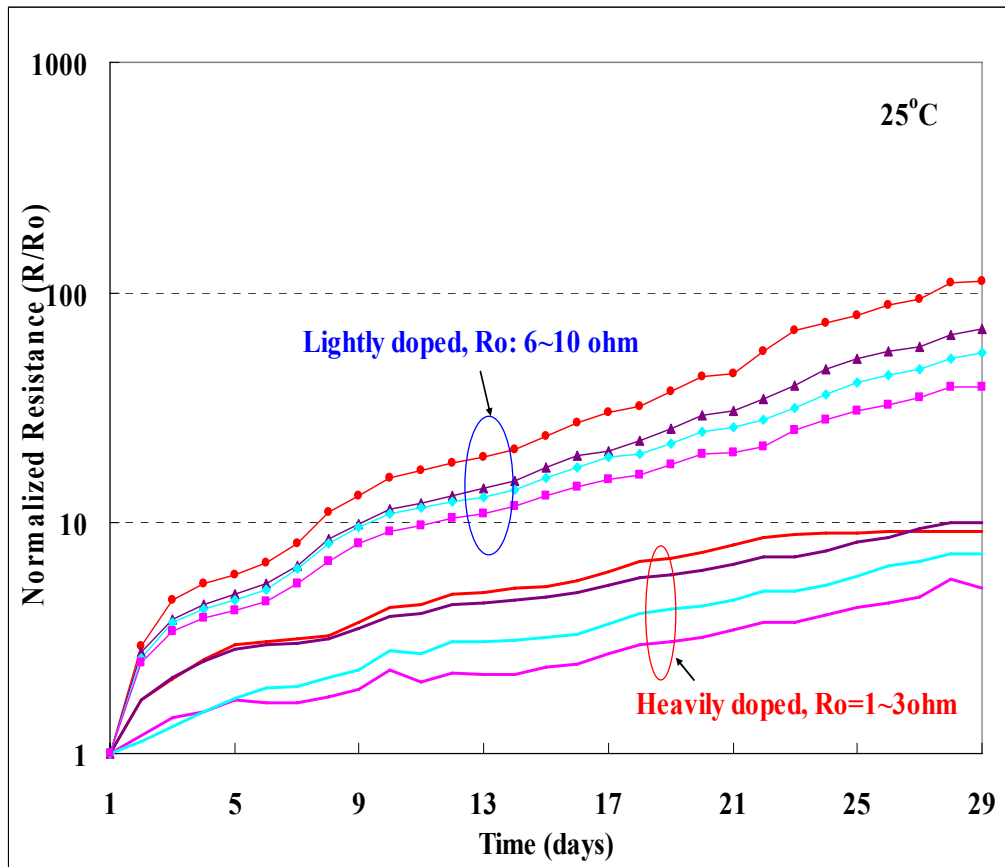
Figure 5-1 Normalized resistance of P3HT thin film micro-sensor as a function of time, at 25°C, ambient pressure. Some of the sensors were heavily doped to 1~3 Ω while some are lightly doped to 6~10 Ω
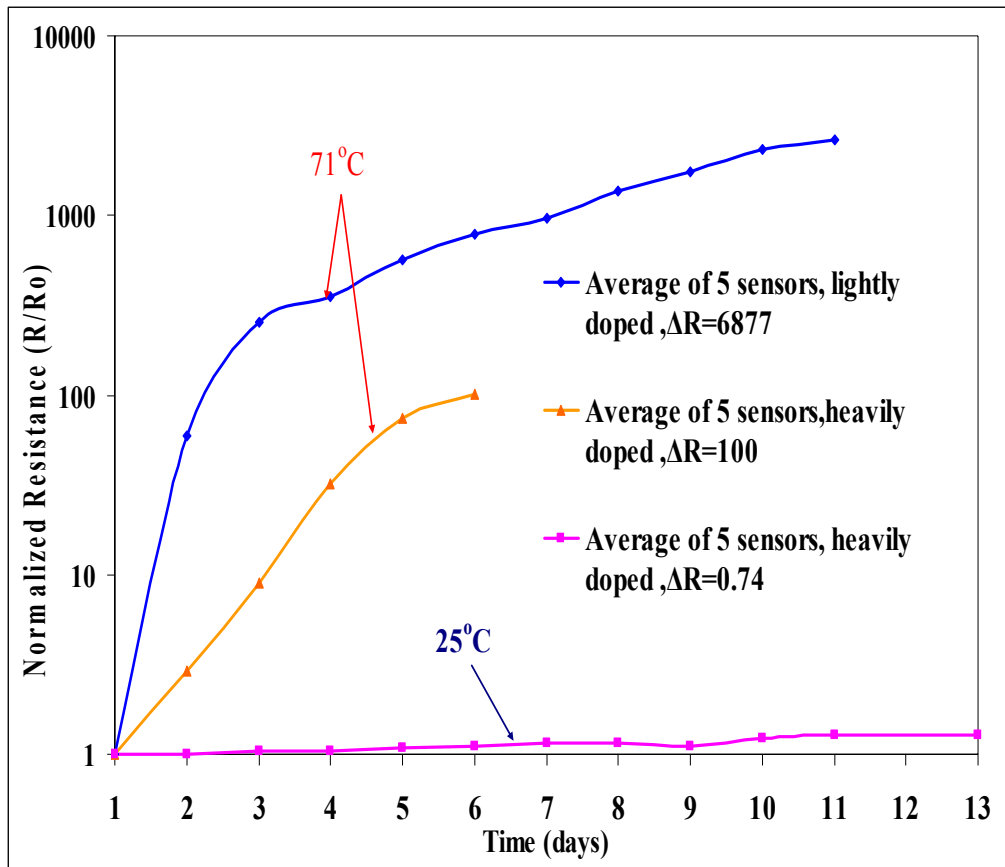
Figure 5-2 Comparison of normalized resistance of P3HT thin film micro-sensor as a function of time at 71°C and 25 °C. All the sensors were doped to less than 6Ω.

Table 5-1   Test conditions for no heat treatment sensors, $25^{o}C$

Sample	Temp (^{o}C)	Doping level	Ro
1	25	Lightly doped	9.3
2	25	Lightly doped	8.5
3	25	Lightly doped	7.8
4	25	Lightly doped	6.4
5	25	Heavily doped	2.8
6	25	Heavily doped	2.1
7	25	Heavily doped	1.6
8	25	Heavily doped	1.4

Table 5-2   Test conditions for no heat treatment sensors at different temperature

Sample	Temp (^{o}C)	Doping level	Ro
1	71	Lightly doped	4.5
2	71	Lightly doped	5.1
3	71	Lightly doped	5.6
4	71	Lightly doped	4.3
5	71	Lightly doped	4.6
6	71	Heavily doped	1.5
7	71	Heavily doped	1.6
8	71	Heavily doped	1.4
9	71	Heavily doped	1.5
10	71	Heavily doped	1.5
11	25	Heavily doped	1.4
12	25	Heavily doped	1.4
13	25	Heavily doped	1.5
14	25	Heavily doped	1.6
15	25	Heavily doped	1.5

change since the doped polymer was partially regenerated and the temperature was not high enough to reverse the doping (oxidation) process entirely. Sensors doped to lower initial resistances ($\sim 1\ \Omega$) had better stability or less degradation in the conductivity of P3HT films than sensors doped to higher resistance ($\sim 10\ \Omega$). Therefore, the results suggest that stability, can be further improved by increasing the dopant concentration (decreasing initial resistance). Table 5-1 and Table 5-2 list all the test conditions for each sample.

5.2   Stability Tests with Annealed Micro-sensor

Thermal annealing studies were conducted to investigate the effect of thermal annealing treatments on the long term stability of the P3HT sensors. Figure 5-3 and Figure 5-4 separately show stability test results at 25°C and 71°C. All the micro-sensors were heavily doped to around $1\ \Omega$ as the starting resistance. At room temperature, the resistance change of heavily doped, annealed sensors was less than the no heat treatment sensors after 6 days (Figure 5-3).

In the 71°C stability test, sensors separately annealed at 150°C, 160°C, and 190°C for 1 hour were used to investigate the difference in resistance change with elevated annealing temperature. The environmental humidity was also recorded to study the effect of humidity on the performance of micro-sensor. The results shown in Figure 5-4 indicate that: (1) annealed sensors had much less resistance change than no treatment sensors; (2) thermal annealing improved the sensor's thermal stability at high temperature; (3) small changes in the environmental humidity didn't have an obvious effect on sensor's resistance change; and (4) the correlation between annealing temperature and

84

resistance change of the doped P3HT, thin film, micro-sensor is not clear, which may be due to the influence of different properties of each micro-fabricated sensor. Table 5-2 and Table 5-3 list all the test conditions for each tested samples.
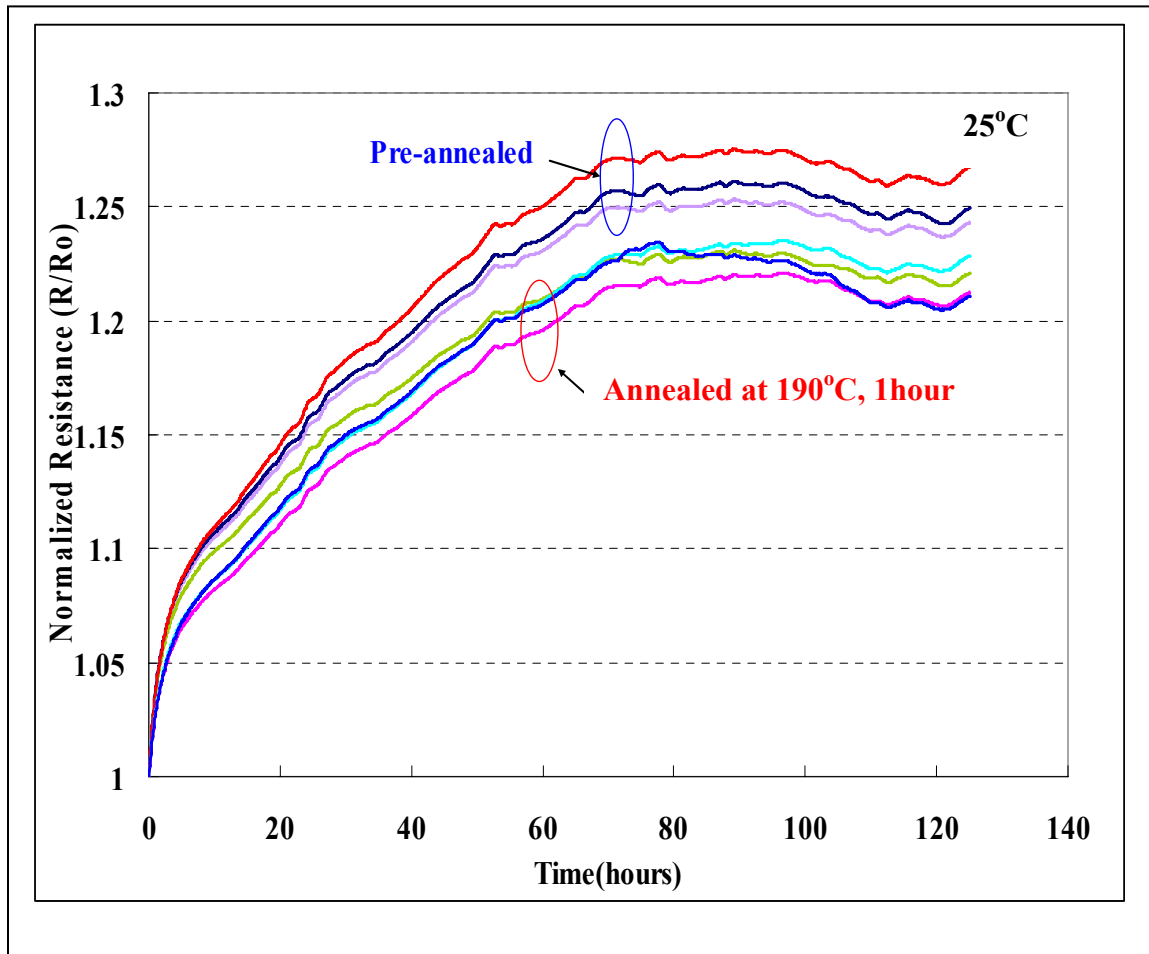
Figure 5-3   Comparison of normalized resistance of not treated and annealed (190°C-1h) P3HT thin film micro-sensor as a function of time at 25 ^{o}C. All the sensors were heavily doped to around 1.5 Ω.
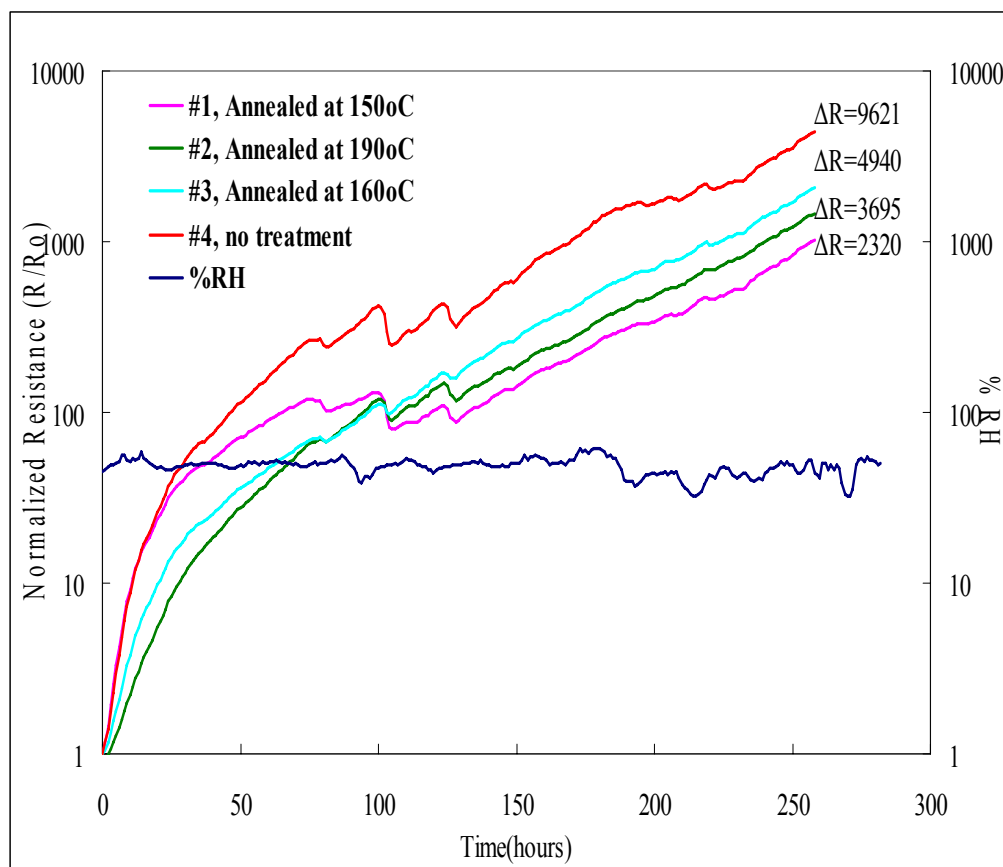
Figure 5-4   Comparison of normalized resistance of no treatment and annealed ($150\,^{\circ}$C, $160\,^{\circ}$C, $190\,^{\circ}$C for 1 hour) P3HT thin film micro-sensor as a function of time at $71\,^{\circ}$C, in air with around 80% RH. All the sensors were heavily doped to around 1.5 Ω.

Table 5-3   Test conditions for annealed and no treatment sensors, 25°C

Sample	Temp ($^{\circ}$C)	Heat treatment	Ro
1	25	no	1.4
2	25	no	1.5
3	25	no	1.5
4	25	190°C-1h	1.4
5	25	190°C-1h	1.5
6	25	190°C-1h	1.5
7	25	190°C-1h	1.4

Table 5-4   Test conditions for annealed and no treatment sensors, 71°C

Sample	Temp ($^{\circ}$C)	Heat treatment	Ro
1	71	150°C-1h	1.5
2	71	190°C-1h	1.5
3	71	160°C-1h	1.4
4	71	No treatment	1.5

CHAPTER 6

CONCLUSIONS

Electrically conducting Poly (3-Hexylthiophene) thin films were investigated for possible use as a chemiresistor micro-sensor for hydrazine/MMH vapor detection at part-per-million and part-per-billion concentration levels. The P3HT thin films (200nm) were spin coated onto a silicon substrate with interdigitated gold electrodes to form the micro-sensor. The change in resistance of P-type doped P3HT thin film due to the interaction with reducing hydrazine is utilized as the principle of operation for the sensor. Upon exposure to 25 ppm hydrazine/MMH, the sensor's resistance changed from a few ohms (1-9 ohms) to over a megaohm (1-50 x 10^6 ohms). This large and easily measured response depends mainly on the hydrazine concentration with a secondary dependence on environmental temperature. This research determined that the properties of the sensor can be modified by annealing and doping changes that affect the structure and therefore the performance of the sensor. The performance of the P3HT thin film micro-sensor can be summarized as:

1. Upon exposure to 25 ppm hydrazine/MMH, the sensor's resistance permanently changed from a few ohms (1-9 ohms) to over a megaohm (1-50 x 10^6 ohms) within minutes.

2. The micro-sensor is capable of sensing hydrazine vapor at low part-per-billion levels. The response rate can be enhanced by thermally heat treating the micro-sensors during fabrication.

3. The room temperature performance of heavily doped sensors is much more stable after long time storage than lightly doped sensors. The thermal stability of heavily doped sensors at high temperature can be improved by thermal annealing.

4. Microstructural alignment of P3HT has occurred during the annealing process, as the average crystallite size became larger for each P3HT film after heat-treatment. The sensor's performance can be improved by thermal annealing treatment.

5. Annealing should be one of the process steps in the fabrication of conducting polymer devices.

In the future work, more research must be focused on the improvement on several parts such as sensor's reliability, sensor's response rate to hydrazine gas at very low ppb concentration levels (1ppb ~ 20ppb), response rate of packaged sensor to hydrazine gas, and the multiple sensors on the single stage.

BIBLIOGRAPHY

1.   M. C. Lonergan, E. J. Severin, B.J. Doleman, S. A. Beaber, R. H. Grubbs, and N. S. Lewis, "Array-Based Vapor Sensing Using Chemically Sensitive, Carbon Black-Polymer Resistors," *Chem. Materials,* v 8, n 9, 1996, p 2298.

2.   J. W. Gardner, T. C. Pearce, S. Friel, P. N. Bartlett, and N. Blair, "A Multisensor System for Beer Flavor Monitoring Using an Array of Conducting Polymers and Predictive Classifiers," *Sensors and Actuators, B: Chemical*, v B18, n 1-3 pt 1, 1994, p 240-243

3.   M. A. Ryan, M. L. Homer, M. G. Buehler, K. S. Manatt, F. Zee, and J. Graf, "Monitoring the Air Quality in a Closed Chamber Using an Electronic Nose," *Proceedings of the International Conference on Environmental Systems,* Society of Automotive Engineers, Lake Tahoe, Nevada, 1997.

4.   D. R. Turner, *Proceedings of the Symposium on Chemical Sensors*, 87-9, Pennington, NJ, The Electrochemical Society, 1987.

5.   R.W. Murray, R. E. Dessy, W. R. Heineman, J. Janata, W. R. Seitz, eds., *Chemical Sensors and Microinstrumentation*, American Chemical Society, Washington, D.C., 1989.

6.   J. W. Gardner, *Microsensors Principles and Applications*, John Wiley & Son, 1994.

7.   Tetsuro Seiyama, *Chemical Senor Technology*, Tokyo: Kodansha; New York: Elsevier, Vol. 1, 1988.

8.   C. E. Davis, C. K. Ho, R. C. Hughes, and M. L. Thomas, "Enhanced detection of *m*-xylene using a preconcentrator with a chemiresistor sensor," *Sensors and Actuators B* 104, 2005, p 207–216.

9.   D. L. Ellis, "Investigation of Thin Film sensor Based on Conducting Polymers," in Chemistry department, Harvard University, 1993.

10.   J. E. Frommer, R. R. Chance, *Encyclopedia of Polymer Science and Engineering*, Vol. 5, Wiley: New York, 1986.

11.   J. W. Gardner, P. N. Bartlett, "Application of conducting polymer technology in Microsystems," *Sensors and Actuators A*, 51, 1995, p 57-66.

12.   M. F. Rubber, "Conjugated Polymeric Conductors" in Molecular Electronics," J. Ashwell(Ed.), Research Studies Press LTD, John Wiley and Sons, 65, 1992.

13.   J. Roncali, "Conjugated Poly(thiophenes). Synthesis, functionalization, and applications," *Chemical Reviews*, 92, 4, 1992, p 711.

14.   T. Skotheim, *Handbook of Conducting Polymers,* volume 1, 2, Marcel Dekker: New York, 1986.

15.   www.answers.com/topic/polythiophene#wp-endnote_McCullough_etal_1993

16.   Gerard Bidan, "Electroconducting conjugated polymers: new sensitive matrices to build up chemical or electrochemical sensors. A review," *Sensors and Actuators, B: hemical*, B6, n 1-3, 1992, p 45-56

17.   J. W. Gardner, P. N. Bartlett, *Electronic Noses Principles and Applications*, Oxford, 1999.

18.   T. A. Skotheim, *Handbook of Conducting Polymers*, Dekker, New York, 1986.

19.   Janata, Jiri, Josowicz, Mira, "Conducting Polymers in electronic chemical sensors," *Nature Materials*, 2, n 1, 2003, p 19-24.

20.   Cao Ye, Zhang Guangyou, Hu Wenxiang, Gao Guanghuang, "Multiple-Channel Instrument development for a hypergolic vapour detection," *Chemical Journal on Internet*, 4, 2002, p5.

21.   E. W. Schmidt, *Hydrazine and Its Derivatives: Preparation, Properties, Applications*, 1, Wiley-Interscience, 2001.

22.   Rounbehler, P. David, "Detection of hydrazine compounds in gaseous samples by their conversion to nitric oxide-yielding derivatives," United Patent 4775653, 1988.

23.   Rose-Pehrsson, Susan, Collins, E. Gregory, "Fluorescent detection of hydrazine, monomethylhydrazine, and 1,1-dimethylhydrazine by derivatization with aromatic dicarboxaldehydes," United Patent 5719061,1998.

24.   Z. N. Bao, A. Dodabalapur, A. J. Lovinger, "Soluble and processable regioregular poly(3-hexylthiophene) for thin film field-effect transistor applications with high mobility," *Applied Physics Letters*, 69, n 26, 1996, p 4108.

25.   H. Sirringhaus, N. Tessler, R. H. Friend, *Science*, 1998, 280, p 1741-1744.

26.   N. Stutzmann, R. H. Friend, H. Sirringhaus, *Science*, 299, 2003, p1881-1884.

27.   Dicker, Gerald, M. P. De Haas, J. M. Warman, D. M. De Leeuw, L. D. A, Siebbeles, "The disperse charge-carrier kinetics in regioregular poly(3-hexylthiophene)," *Journal of Physical Chemistry B*, 108, n 46, 2004, p17818-17824

28.   T. Chen, X. Wu, and R. D. Rieke, "Regiocontrolled Synthesis of Poly (3-alkylthiophenes) Mediated by Rieke Zinc: Their Characterization and Solid-State Properties," Journal of American Chemistry Society, 117,1995, p 233-244.

29.   R. Osterbacka, C. P. An, X. M. Jiang, Z. V. Vardeny, "Two-dimensional electronic excitations in self-assembled conjugated polymer nanocrystals," *Science*, 287, n 5454, 2000, p 839-842.

30.   H. Yang, "Study of Poly (3-hexylthiophene) Conducting Polymer Thin Film Micro-Sensor For Hydrazine Vapor Detection," Auburn University, 2004.

31.   M. S. A. Abdou, F. P. Orfino, Y. Son, S. Holdcroft, "Interaction of oxygen with conjugated polymers: Charge transfer complex formation with poly(3-alkylthiophenes)," *Journal of the American Chemical Society*, 119, n 19, 1997, p 4518.

32.   H. Sirringhaus, N. Tessler, D. S. Thomas, P. J. Brown, and R. H. Friend, *Advances in Solid State Physics*, edited by B. Kramer (Vieweg, Braunschweig, 1999), 39, p 101.

33.   J. Ficker, H. von Seggern, H. Rost, W. Fix, W. Clemens, and I. McCulloch, "Influence of intensive light exposure on polymer field-effect transistors," *Applied Physics Letters*, 85, n 8, 2004, p 1377-1379.

34.   B. S. Ong, Y. L. Wu, P. Liu, S. Gardner, "High-Performance Semiconducting Polythiophenes for Organic Thin-Film Transistors," *Journal of the American Chemical Society*, 126, n 11, 2004, p 3378-3379.

35.   R. Jaeger, *Introduction to Micro Electronic Fabrication*, Addison-Wesley Publishing, Inc.1988.

36.   W. R. Runyan, *Semiconductor measurements and Instrumentation*, McGrawHill, New York, 1975.

37.   S. K. Ghandhi, *The Theory and Practice of Microelectronics*, John Wiley & Sons, New York, 1968.

38.   H. Sirringhaus, P. J. Brown, R. H. Friend, M. H. Nielsen, K. Bechgaard, B. M. W. Langeveld-Voss, A. J. H. Spiering, R. A. J. Janssen, E. W. Meijer, P. Herwig, D. M. de Leeuw, "Two-dimensional charge transport in self-organized, high-mobility conjugated polymers," *Nature*, 401, n 6754, 1999, p 685-688.

39.   G. Kilic, L. Toppare, E. Yurtsever, " Studies of polythiophenes," *Synthetic Metals*, v 78, n 1, 1996, p 19-25.